SEDIMENTOLOGY the journal of the International Association of Sedimentologists IAS

Sedimentology (2024) **71**, 850–870 doi: 10.1111/sed.13153

Microbialites on the northern shelf of Lake Van, eastern Türkiye[#]: Morphology, texture, stable isotope geochemistry and age

M. NAMIK ÇAĞATAY*, EMRE DAMCI*,[1], GERMAIN BAYON† and MUSTAFA SARI‡

**Faculty of Mining, EMCOL Research Centre, İstanbul Teknik Üniversitesi, Maslak, İstanbul 34469, Türkiye (E-mail: cagatay@itu.edu.tr)*

†IFREMER, Marine Geosciences Research Unit, Plouzané 29280, France

‡Maritime Faculty, Bandırma Onyedi Eylül Üniversitesi, Bandırma, Balıkesir 10200, Türkiye

Associate Editor – Mike Rogerson

ABSTRACT

Lake Van, the world's largest alkaline lake, hosts some of the largest microbialite towers worldwide, which are considered as modern analogues of ancient stromatolites. This study investigates the links between microbialite evolution, geology, climate and hydrology, and the role of biotic and abiotic processes in microbialite growth and morphology. For these objectives, the northern shelf of Lake Van was surveyed by sub-bottom seismic profiling and diving, and two 9 m and 15 m high microbialite chimneys were sampled at 25 m water depth. Samples were analysed for stable oxygen and carbon isotopes, X-ray diffractometry, scanning electron microscopy and U/Th age dating. Lake Van microbialites precipitate wherever focused Ca-rich groundwater flows onto the lake floor to mix with alkaline lake water. Variable columnar, conical and branching morphologies of the microbialites indicate various processes of formation by groundwater channelling within the chimneys. Collectively, our data suggest that the microbialite chimneys have formed within the last millennium, most likely starting during the warm and humid Medieval Climate Anomaly (*ca* AD 800–1300), when lake level rose approximately to the present level due to enhanced Inputs of riverine Ca-rich freshwater and groundwater. Our new scanning electron microscopy observations indicate that the internal structure of the microbialites below the outer cyanobacteria-covered crust is constructed by calcified filaments, globular aggregates and nanocrystals of algal, cyanobacterial and heterobacterial origins and inorganically precipitated prismatic calcite crystals. These textural features, together with dive observations, clearly demonstrate the important role of inorganic carbonate precipitation at sites of groundwater discharge, followed by cyanobacteria and algal mucilage deposition and microbially meditated calcification in the photic zone in the rapid growth of the microbialite chimneys. Considering the close similarities of some textures with those of ancient stromatolites and meteorites, the results of this study provide new insights into the environmental conditions associated with stromatolite formation and extra-terrestrial life evolution.

[1]Present address: Sis Enerji Üretim A.Ş. Sahil Yolu Cd. Turgut Özal Bulvarı, No. 65. Küçükyalı, Maltepe, İstanbul, Türkiye

[#]Note that Türkiye is the new registered official name of the country, replacing Turkey.

Keywords Lake Van, microbialite, mineral and isotopic compositions, morphology, textures, Türkiye, U/Th ages.

INTRODUCTION

Some of the largest microbialites worldwide occur in Lake Van (Eastern Turkey), the largest soda lake on Earth characterized by an alkalinity of 155 mM and pH of 9.7 to 9.8 (Kempe *et al.*, 1991; Reimer *et al.*, 2009) (Fig. 1A). Lake Van microbialites have been identified using sub-bottom seismic profiling and underwater photography in nearshore shelf areas up to 130 m water depth, occurring as chimneys, columns, towers or spires that rise up to 35 m above the lake floor (Figs 1B, r1C and 2) (Kempe *et al.*, 1991; Cukur *et al.*, 2015, this study). These microbialites display some morphological similarities with the tufa towers from the soda and saline lakes of the Basin and Range Province (Bischoff *et al.*, 1993; Rosen *et al.*, 2004) and chimney-like carbonates that have been observed in alkaline salty lakes of the Afar Rift in East Africa (Dekov *et al.*, 2014).

Microbialites are generally considered as modern analogues of stromatolites, which appeared in the geobiological sediment record as early as the Archaean (Grotzinger & Knoll, 1999; Kazmierczak & Altermnn, 2002; Reitner *et al.*, 2011). Hence, investigation of modern microbialites provides important information on debated issues related to the formation and evolution of stromatolites and early benthic habitats over Earth history. Cyanobacterial and photosynthetic activity have long been regarded as the main driving forces in the formation of microbialites and stromatolites, associated with carbonate supersaturation and precipitation (e.g. Riding, 1982; Pentecost & Bauld, 1988; Merz, 1992). However, more recent studies have suggested that heterotrophic bacteria could also play a pivotal role in the mineralization of extracellular polymeric substances (EPS) of cyanobacterial origin during the formation of microbialites and stromatolites (Chafetz & Buczynski, 1992; Knorre & Krumbein, 2000; Arp *et al.*, 2001; Paerl & Reid, 2001; Altermann, 2004; Couradeau *et al.*, 2013; Brasier *et al.*, 2018; Kremer *et al.*, 2019).

Microbialites (and their ancient analogues, stromatolites) are hypothesized to form under favourable environmental conditions and, hence, can be used as proxies for palaeoclimatic and physicochemical conditions, such as lake levels and carbonate saturation state (e.g. Awramik & Buchheim, 2015; Yeşilova *et al.*, 2019; Ingalls *et al.*, 2022). Recently, Ca and Mg/Ca carbonate-rich microbialites from soda lakes such as lakes Van and Salda in Turkey have been compared with similar deposits from Mars; hence their being interpreted in the context of Martian life evolution (López-García *et al.*, 2005; Michalski *et al.*, 2017; Salvatore *et al.*, 2018; Balci *et al.*, 2020). In particular, some nano-size (0.05–0.15 μm in diameter) carbonate globules found in microbialites and meteorites, including the famous Martian ALH84001 meteorite and the Tatahouine meteorite, are believed to represent fossil traces of 'nanobacteria' (Folk, 1993; Pedone & Folk, 1996; Benzerara *et al.*, 2003; Kazmierczak & Kempe, 2003; Kazmierczak *et al.*, 2004; López-García *et al.*, 2005; Kremer *et al.*, 2018; Balci *et al.*, 2020). Recent discovery that microbialite-bearing units in ancient lacustrine successions, such as the Lower Cretaceous 'pre-salt' formations in offshore Brazil and Angola (Wright & Barnett, 2015), are economically important as hydrocarbon reservoirs has raised further interest in modern microbialites studies.

Since their initial discovery in Lake Van by Kempe *et al.* (1991), subaqueous microbialites have been studied at various scales, from nano-metre to macro-metre investigation, using multi-disciplinary methods. These include field studies to delineate the areal distribution of submerged microbialites, using multi-beam and high-resolution seismic data (Cukur *et al.*, 2015; this study), and various laboratory analyses to characterize their molecular, organic and inorganic chemical and mineralogical composition, using optical microscopy, scanning electron microscopy (SEM), energy dispersive X-ray spectrometry (EDS), scanning transmission X-ray microscopy (STXM) and X-ray diffraction (XRD) (López-García *et al.*, 2005; Benzerara *et al.*, 2006; Kremer *et al.*, 2019). The overall conclusion of these studies is that Lake Van microbilolites were formed by carbonate and silicate mineralization of cynobacterial mats and biofilms, induced by mixing between Ca–Fe–Si-enriched spring waters emerging from the lake floor and the alkaline lake waters, with reactions being

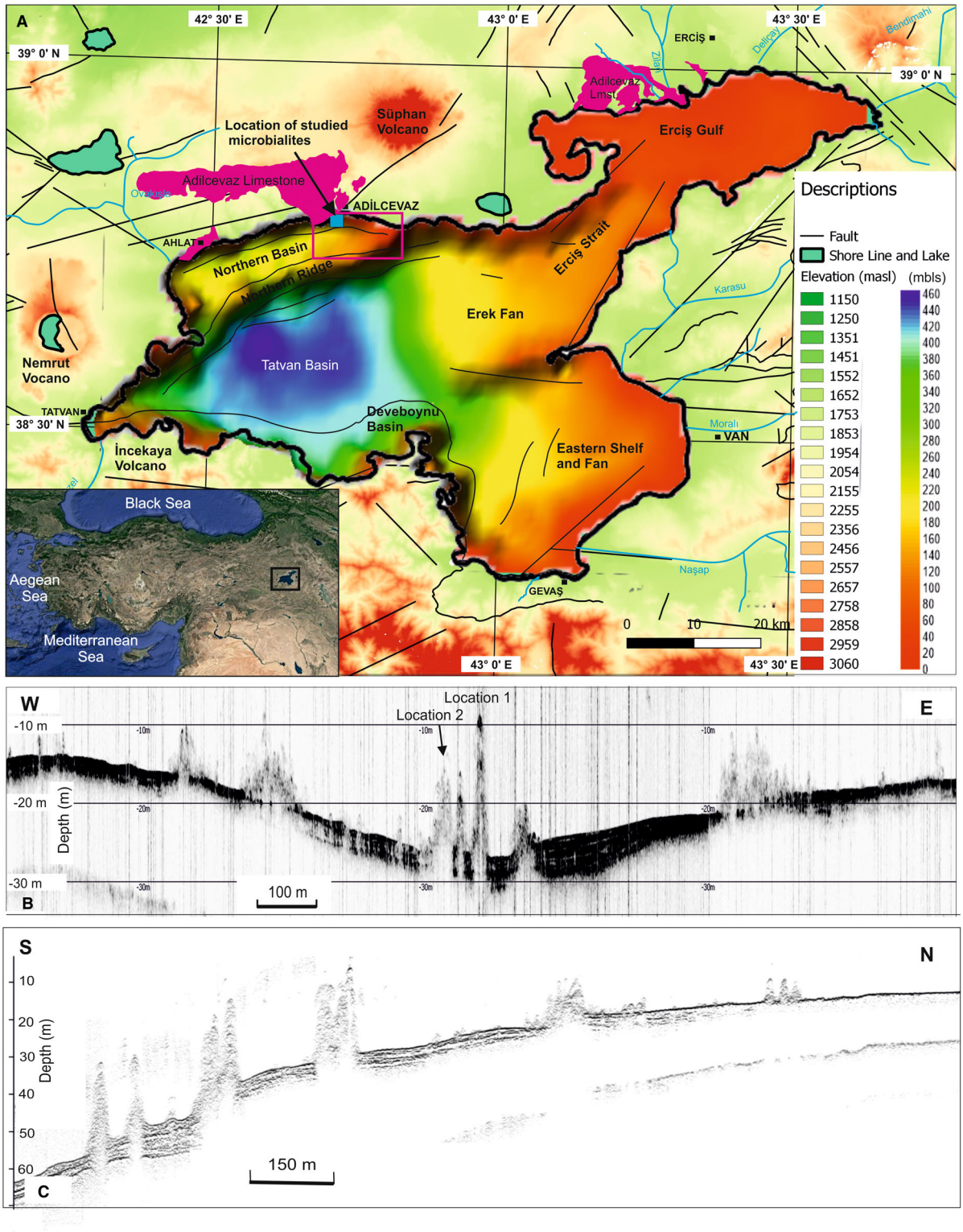

Fig. 1. (A) Bathymetry map of Lake Van showing the various morphological regions. The area off Adilcevaz Town surveyed by sub-bottom seismic profiling is outlined by a red rectangle and the area where the two microbialites were sampled is shown with a blue infilled square. Note the outcrops of Miocene Adilcevaz Limestone (in purple) on the onshore areas. (B) and (C) West–east and south–north sub-bottom profile showing the microbialites, including the sampled ones in (B). Note that microbialites emerge from up to 5 m thick sediments.

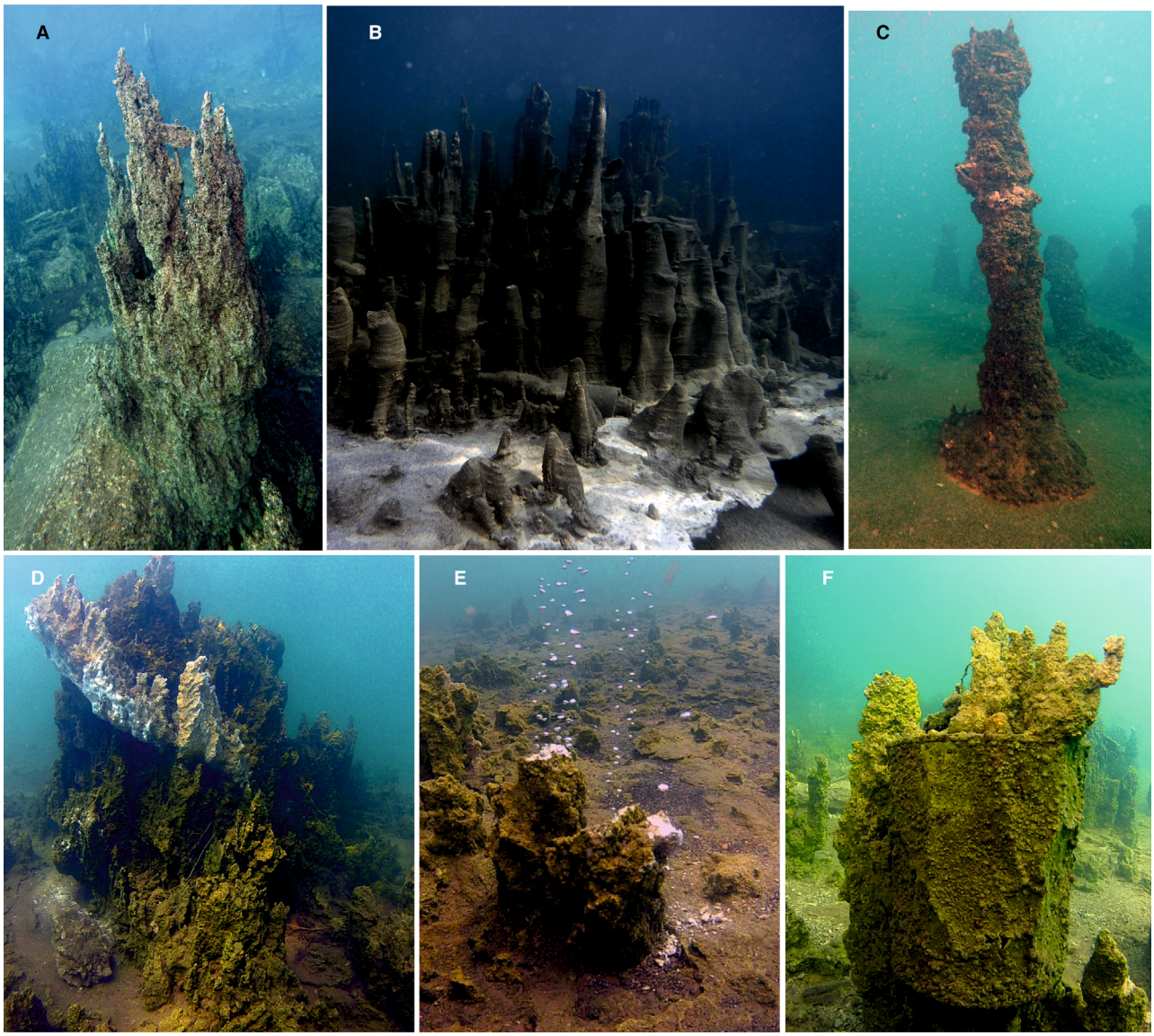

Fig. 2. Underwater photographs of microbialites off Adilcevaz Town: (A) A 1.7 m high tree-like branching microbialite at a water depth of 13 m. (B) A swarm of 0.3 m to 1.0 m high conical microbialites developed on a white carbonate substrate; water depth: *ca* 3 m. (C) A 3 m high columnar microbialite situated on a sand substrate; water depth: *ca* 10 m. (D) A 2.5 m high microbialite chimney at 4.5 m water depth. Note the two parts of the microbialite: a dark green cyanobacterial coated main part below; and white, newly formed feather-like carbonate growths with partly mineralized brown patches above. See a video of this chimney at: http://www.emcol.itu.edu.tr/Icerik.aspx?sid=13881. (E) Two *ca* 0.35 m high microbialite chimneys emitting freshwater and gas bubbles in the water column. Note the white soft precipitates atop microbialite and nearby lake floor encrusted with carbonate crust; water depth: 4.5 m. (F) A recently formed 0.5 m high microbialite chimney engulfing a 0.3 m high food can; water depth: *ca* 4.5 m. The can is estimated to be not more than a few tens of years old.

mediated by the heterotrophic bacterial metabolism of cyanobacteria.

However, some important issues, including links between microbialite evolution, climate and hydrology, and the role of biotic and abiotic processes in microbialites growth and morphology, have not been unequivocally established in Lake Van and other alkaline, saline lakes, such as Mono Lake, California, and Afar, east Africa. For example, there are still conflicting reports on the relationships between microbialite growth and lake level (i.e. transgressions versus regressions). Some

studies report the importance of lacustrine regression for the development of tufa chimneys (for example, Eocene Green River Formation; Ingalls *et al.*, 2022), whereas others favour the transgressions and high lake levels (for example, Lake Van: Yeşilova *et al.*, 2019; Green River Formation: Awramik & Buchheim, 2015; Mono Lake: Keevil *et al.*, 2022). Similarly, some models of tufa chimney growth in alkaline lakes are biased towards assuming a prevalence of abiotic processes (for example, Mono Lake: Council & Bennett, 1993; Afar Rift: Dekov *et al.*, 2014), while others stress the importance of biotic processes (e.g. Arp *et al.*, 2001; Paerl & Reid, 2001; Rogerson *et al.*, 2008; Couradeau *et al.*, 2013; Gerard *et al.*, 2013; Brasier *et al.*, 2018; Kremer *et al.*, 2019).

The present study aims to address these issues by reporting new results of field and laboratory investigations on submerged microbialites from the northern shelf of Lake Van, off Adilcevaz Town (Fig. 1A). These results include: (i) the first long-term dive observations and seismic data on the distribution, morphology and growth of the microbialites; (ii) scanning electron microscope (SEM) and X-ray diffraction (XRD) data on biotic and abiotic textures and mineral composition; (iii) the first set of stable carbon and oxygen data on the sources of waters involved in microbialite precipitation; and (iv) the first set of U/Th age data, used to constrain the ages of microbialites and discuss their temporal evolution. Based on these field observations and analytical data, this article discusses the importance of the environmental (geological, limnological, climatic) factors and mineralization processes in the formation of Lake Van microbialites, which provide insight into critical palaeoenvironmental and physicochemical factors, and biotic and abiotic processes responsible for the formation of modern microbialites and their ancient analogues (stromatolites).

LAKE VAN: PHYSIOGRAPHIC, GEOLOGICAL AND HYDROLOGICAL SETTINGS

Lake Van is a terminal lake and the largest soda lake in the world, with a volume of 607 km^3, area of 3712 km^2 and a maximum depth of 451 m. The lake is located on the East Anatolian Plateau in eastern Turkey, at an altitude of 1648 m above sea level (masl) (Fig. 1A). The lake consists of the 450 m deep Tatvan Basin, the *ca* 410 m deep small Ahlat sub-basin and the 260 m deep Northern Basin, and the dividing ridges and surrounding shelf areas have <150 m water depth (Cukur *et al.*, 2015). Submerged microbialites are common topographic features of the shelf areas off Van, Gevaş, Muradiye, Erciş, Adilcevaz, Ahlat, Tatvan and Reşadiye towns, occurring as swarms of tree-like buildups in sub-bottom seismic profiles and underwater photographs (Figs 1B, 1C and 2; Wong & Finckh, 1978; Kempe *et al.*, 1991; Cukur *et al.*, 2015; Kremer *et al.*, 2019). In the northern shelf, microbialites are observed at water depths ranging from a few metres to −130 m. They also occur onshore, up to 75 m above the current lake level (Yeşilova *et al.*, 2019).

The lake catchment includes Quaternary volcanic and Lower Miocene marine carbonates in the west and north, marbles and other metasedimentary rocks of the Bitlis Massif in the south, and Pliocene sedimentary rocks in the east (Fig. 1A). The Van region is characterized by a continental climate with cold and wet winters and warm and dry summers. Surface water temperatures range from 21 to 25°C in summer and 2 to 7°C in winter (Kavak & Karadogan, 2012).

The lake water has a pH of 9.81 and alkalinity of 155 mM. It is of Na–CO3–Cl–(SO4) type with low Ca (*ca* 0.19 meq/L) and relatively high Mg (*ca* 9.0 meq/L) concentrations and high Mg/Ca (*ca* 45) (Reimer *et al.*, 2009). The lake water is oversaturated with respect to calcite, aragonite and dolomite. Lake Van is presently a monomictic lake, at least convecting partially (Kremer *et al.*, 2019), and is anoxic below 300 m (Kipfer *et al.*, 1994; Reimer *et al.*, 2009; Stockhecke *et al.*, 2012). Summer stratification occurs because of warming of the upper 10 to 15 m surface water layer to 17 to 20°C (Reimer *et al.*, 2009). The temperature decreases to a minimum of *ca* 3°C between 40 m and 50 m water depth, while a slight salinity increase occurs from 21.9 psu from the surface layer to 22.5 psu at 100 m depth. Spring to early summer freshwater influx slightly lowers total salinity and alkalinity in the surface layer. Commonly, biological productivity during spring and summer leads to an increase of pH by CO_2 consumption in the surface layer and pH decrease in the hypolimnion due to organic matter decay. The euphotic zone is 35 m deep for most of the year, except in winter during which it extends to 50 m depth (Huguet *et al.*, 2011). The lake is biologically different from both freshwater and marine ecosystems, and contains 103 phytoplankton taxa, 36 zooplankton and only two endemic fish species (Sarı, 2008; Akkuş *et al.*, 2021).

The annual precipitation in the Van region is *ca* 400 mm/yr, which mostly occurs as winter snow and spring rain and river runoff (Kadıoğlu *et al.*, 1997). The freshwater influx reaches maximum levels in late spring and early summer by snow melting on the surrounding mountains. Inter-annual lake level variations range from a minimum of 1646.69 masl in January 1963 to a maximum of 1650.55 masl in June 1995, with a seasonal variation of 42 cm (E.İ.E.İ., 1996, 2008).

The hydrochemistry of Lake Van, associated rivers and sub-lacustrine spring waters were studied by Reimer *et al.* (2009), and later in the south by Kremer *et al.* (2019). Several rivers and springs discharge freshwater into the lake. The rivers draining carbonate terrain in the west, north-west and south deliver bicarbonate and Ca-rich waters (for example, of Küçüksu, Gevaş, Engil rivers and those in the Adilcevaz area), whereas rivers draining the Quaternary volcanic rocks in the west and north (for example, Süfresor, Zilan, Bendimahi and Deliçay rivers) supply bicarbonate, alkaline elements (Na and K), chloride and sulphate. The river waters have an average molar Mg/Ca of 2 : 1, and are undersaturated with respect to calcite and aragonite (Reimer *et al.*, 2009).

Sub-lacustrine spring waters in the south-west of the lake display average Ca and Mg concentrations of *ca* 3.9 meq/L and 3.1 meq/L, respectively, with an average molar Mg/Ca of 0.79, average pH of 7.5 and alkalinity of 16.16 meq/L (range 54.8 to −0.11 meq/L) (Kremer *et al.*, 2019). The spring waters are mostly undersaturated to slightly oversaturated with respect to carbonate minerals. Their alkaline element contents are commonly higher than those of the river waters. The river mouths in the nearshore areas show milky carbonate (mainly calcite) precipitation (whiting), which is induced by mixing of Ca-rich river waters with the carbonate-rich lake waters. The lake sediments are varved due to lack of benthic activity (e.g. Kempe *et al.*, 2002; Çağatay *et al.*, 2014; Damcı & Çağatay, 2018). Recent confocal Raman microscopy and electron microprobe analysis analyses of the varved sediments by McCormack *et al.* (2019) show that the couplets of Ca-rich (carbonate-rich) light laminae and Si–Mg-rich (siliciclastic rich) dark laminae are enriched in aragonite and calcite, respectively. This result implies the seasonality of the carbonate polymorphs precipitation, mainly in the epilimnion, with calcite precipitating together with siliciclastic detrital input during high spring runoff and aragonite during late summer under conditions of reduced river runoff and high evaporation.

MATERIALS AND METHODS

Seismic survey

The INNOMAR SES 2000 sub-bottom profiler (Innomar Technologie GmbH, Rostock, Germany) was used on a small vessel to acquire seismic data during 2012 (Wunderlich & Müller, 2003). The profiler was operated with an effective frequency 8 kHz with four pulses and gain level set to 60 dB. PowerMax DGPS (CSI Wireless Inc, Calgary, AB, Canada) was used for positioning. A sound velocity of 1500 ms^{-1} was applied in the water. Post-processing of the data was made with the Innomar ISE software v.2.91.

Sampling methods

Two microbialite chimneys were sampled by diving at locations of 38°47′ 43.7″N/ 042°43′ 25.2″E (Location 1) and 38°47′ 43.5”N/042°43′ 24.0″E (Location 2) offshore Adilcevaz town on 31 August 2014 (Fig. 2). The sampled microbialite chimneys 1 and 2 are 15 m and 9 m high respectively, with their summits being located at 6 m and 15 m below the lake level, respectively. Poor visibility due to high turbidity did not allow for underwater photography at the time of sampling. However, one of the co-authors (Mustafa San) performed extensive diving and underwater photography in the study area before and after the field sampling.

Each microbialite was sampled at four different depths: the base, 2 m above the base, and at their middle and upper parts. Each sample consisted of chunks measuring between 40 cm and 60 cm long and 30 to 50 cm wide. The samples were transported to EMCOL Research Centre at Istanbul Technical University, and kept in a freeze dryer until sample preparation and analyses. The samples were cut to observe the internal structure for visual description and the internal carbonate parts, *ca* 10 to 20 cm from the edge, were sub-sampled for binocular microscopy, mineralogical (XRD), SEM, stable isotopic and U/Th age dating analyses.

Petrographic studies

The structure and texture of the microbialite samples were studied and characterized at both

centimetre to micrometre scales, using a binocular microscope and JEOL JSM-7000F scanning electron microscope (SEM; JEOL Limited, Tokyo, Japan) coupled with an energy dispersive X-ray spectrometer (EDS). The samples were coated by platinum before the SEM analyses, and the SEM was operated at 10 kV.

X-ray diffraction analysis

Mineralogical analyses of the samples were carried out a by powder XRD method. A Bruker D8 Advance X-ray diffractometer equipped with a Lynxeye detector was used for the analysis (Bruker, Billerica, MA, USA). The powder samples were mounted on concentrically grooved sample holders made of polymethyl methacrylate (PMMA) having 25 mm diameter. Samples were analysed using Cu Kα radiation, with the power generator operated at 30 kV and 40 mA, and the diffractometer run with $\Delta°2 = 0.00571346$ step-size and 0.1 s scanning speed. The semi-quantitative estimation of the relative calcite and aragonite percentages (as a percentage of 100% total carbonate) was made from the peak heights of main reflections of calcite (d_{104}) at 3.03 Å and aragonite (d_{111}) at 3.39 Å (Goldsmith *et al.*, 1961).

Stable oxygen and carbon isotope analyses

Stable carbon and oxygen isotopic compositions of the carbonates in the microbialite samples were measured using an automated carbonate preparation device (KIEL-III; Thermo Fisher Scientific, Waltham, MA, USA) coupled to a gas-ratio mass spectrometer (Finnigan MAT 252) at the Isotope Geochemistry Laboratory of University of Arizona. Powdered bulk samples were reacted with dehydrated phosphoric acid under vacuum at 70°C. Measured isotope ratios were calibrated based on repeated measurements of NBS-19 and NBS-18, yielding precisions of ±0.1‰ VPDB (Vienna Pee-Dee Belemnite) for $\delta^{18}O$ and ±0.06‰ VPDB for $\delta^{13}C$ (1σ).

Uranium/thorium (U/Th) dating analyses

About 70 mg of powdered microbialite sample, visibly free of shells, shell fragments and detrital minerals, were dissolved in 7.5 M HNO_3 after addition of a mixed $^{236}U/^{229}Th$ spike (Bayon *et al.*, 2015). After centrifugation, undissolved residual fractions were fully digested in a 3 : 1 mixture of HF : HCl solution, and added back into corresponding supernatants for evaporation. Uranium and Th were separated after Fe-oxide co-precipitation using conventional anion exchange techniques (Bayon *et al.*, 2009). Uranium and Th concentrations and isotope ratios were measured with a MC-ICPMS (Neptune; Thermo Fisher Scientific) at the Pôle Spectrométrie Océan (PSO, Brest, France). Uranium–Th age calculations were performed by the isochron method with the ISOPLOT program (v. 3.71, Ludwig, 2008) in order to correct measured ratios from detrital contamination. All calculations have used the half-lives measured by Cheng *et al.* (2000). Two-point isochron ages were calculated using a theoretical end-member containing hydrogenous Th, characterized by $(^{232}Th/^{238}U) = 0.431 \pm 0.2155$ (50%); $(^{230}Th/^{238}U) = 1 \pm 0.5$ and $(^{234}U/^{238}U) = 1 \pm 0.5$, as inferred from samples 1, 2, 3, 4 and 6 to 10. All isochron ages were given an arbitrary 25% error based on previous estimates (Bayon *et al.*, 2013). This arbitrary error corresponds to the external reproducibility on isochron ages estimated from repeated analyses of an in-house authigenic carbonate standard (Bayon *et al.*, 2013).

RESULTS

Distribution and morphology of Adilcevaz microbialites

The sub-bottom profiles show that the submerged microbialites appear as chimneys rising up to *ca* 20 m high from the lake floor on the Adilcevaz shelf area (Fig. 1B and C). They occur as individual chimneys or as swarms of several chimneys in water depths ranging from a few metres to −130 m. The individual towers vary from a few metres to 20 m, and the swarms are up to 300 m wide in their basal parts. In seismic profiles, the microbialites are characterized by strong outer reflections and transparent internal parts (Fig. 1B and C). Their basal parts rise from up to 10 m thick, surrounding layered sediments, with the thickness commonly increasing with depth. The multibeam bathymetric data by Cukur *et al.* (2015) show that the microbialites on the Adilcevaz shelf are aligned along a north-west/south-east direction and east–west directions.

Underwater dive observations on the Adilcevaz shelf indicate a chimney, tower, column and mound morphologies of the microbialites (Fig. 2). In shallow water (>10 m deep), they rise from the lake floor on a flat, hard carbonate crust (Fig. 2B and E) or carbonate-rich sandy

substrate (Fig. 2C and F). Some chimneys show tree-like branching morphology (Fig. 2A, D and F). The chimneys have a central axial and ancillary channels, with radius of several centimetres, from which fresh spring water discharges and causes turbidity due to milky precipitates (Fig. 2E, Video S1 at: http://www.emcol.itu.edu.tr/Icerik.aspx?sid=13881).

Microbialite textures

At hand-specimen scale, studied microbialites display a highly irregular, hard surface with 0.5 to 2.0 cm protruding pinnacles, and are covered by a very dark green to black mat of coccoid cyanobacteria (Figs 2 and 3A). Below the outer surface layer, the internal parts of the microbialites correspond to white to beige, crumbly, porous carbonate material with *ca* 0.5 cm thick, brown folded organic-rich bands with 1 to 2 cm diameter openings (Fig. 3B).

At microscopic scale, the internal white main carbonate part below the dark surficial cyanobacteria layer consists of mineralized mucilage containing 100 to 600 μm long, 10 to 40 μm in diameter worm-like and tubular organic filaments (Figs 4A to C and 5B), abundant diatom frustules (Fig. 5A), 30 to 40 μm calcareous globules (Fig. 6A to C) and euhedral calcite crystals (Fig. 6B and D). The calcified organic filaments commonly occur as bundles in samples from the basal part of microbialite chimneys (Fig. 4C). They have an axial tube (3 to 7 μm in diameter) that is rimmed by radial growth of calcite crystals. The globules occur as aggregates with their surface covered by fine cellular (<1 μm) growths of cyanobacteria (Fig. 6A to C). The globules have a concentric internal structure, formed by radial growths of calcite, and often include diatom frustules (Fig. 6C). Dogtooth, prismatic calcite crystals protrude between the globule aggregates (Fig. 6B and D). Nano-crystals (<1 μm) of aragonite and rare *ca* 5 μm platelets of hydromagnesite forming alveolar or honeycomb texture are observed under the SEM (Fig. 5).

Mineralogy

Six samples from the two studied microbialite chimneys were analysed by XRD. The samples essentially consist of calcite and aragonite (Fig. S1). The d_{104}-spacing of calcite in Lake Van microbialites has a range of 3.019 to 3.027 Å, which is within the range of 3.015 to 3.035 Å for low-Mg calcite (Goldsmith *et al.*, 1961) (Table 1). Low-Mg calcite is the dominant mineral phase, forming between 80% and 98% (average: 87.5%) of the total carbonate minerals. At Location 2, the relative percentage of low-Mg calcite decreases from the base to the top of the microbialite chimney. However, the upper part of the chimney at Location 1 has a relatively higher low-Mg calcite percentage of 93%. Note that hydromagnesite, while being observed

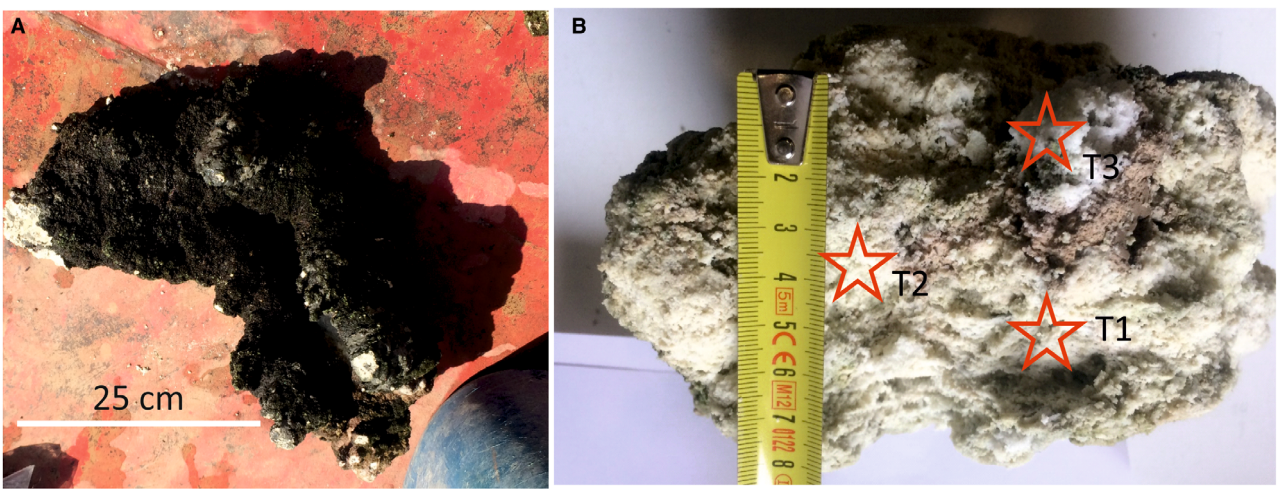

Fig. 3. (A) Irregular surface of microbialite sample covered with very dark green to black sheath of coccoid cyanobacteria, Location 1, middle part. (B) Internal part of microbialite sample below the dark surficial layer. Location 1, basal part. Note the brown, organic matter-rich (EPS) parts. Stars indicate location of sub-samples used for U/Th dating analysis (Table S1).

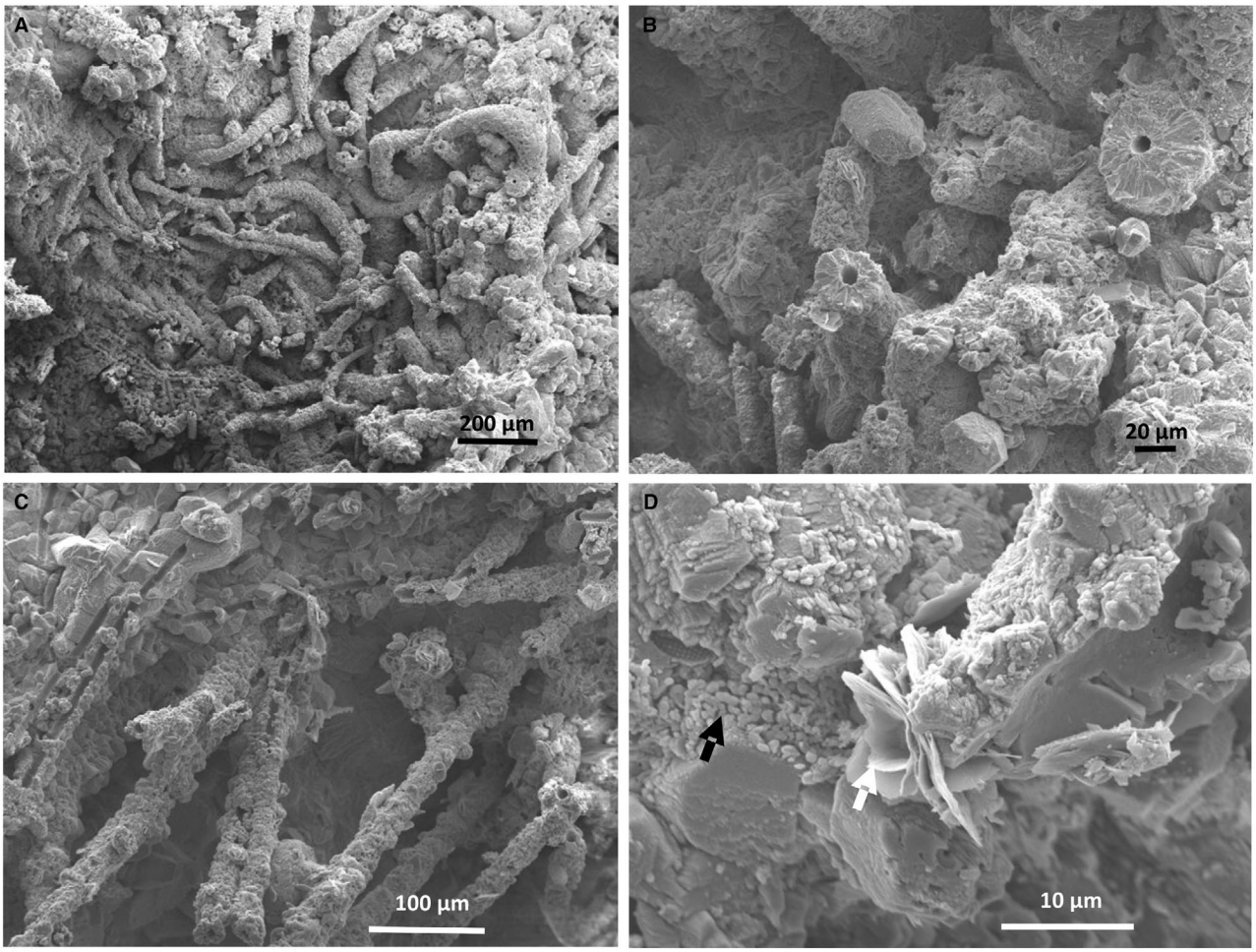

Fig. 4. Scanning electron microscopy (SEM) photomicrographs showing microbialite textures of a sample Van-MB-2-3, lower part, Location 2. (A) Calcified tubular organic filaments and carbonate matrix. (B) Close up view of the organic filaments with calcified radial internal structure. (C) Bundle of calcified organic matter (mucilage). (D) Bacteriogenic nano-crystals of aragonite (black arrow) and platelets of hydromagnesite (white arrow) forming alveolar or honeycomb texture.

under SEM in trace to minor amounts (Fig. 4D), was not detected in the X-ray diffractograms (Fig. S1).

Stable oxygen and carbon isotopes

The $\delta^{18}O$ composition of the bulk carbonates in microbialites ranges from −5.68 to −2.90‰ VPDB (average: −4.30‰ VPDB), while $\delta^{13}C$ ratios vary from 1.91 to 3.43‰ VPDB (average: 2.96‰ VPDB) (Table 2). The $\delta^{18}O$ values of the microbialite chimney at Location 2 were lower (average: −4.97‰ VPDB) than those at Location 1 (average: −3.47‰ VPDB). No systematic change in isotopic compositions was observed along the height of the studied microbialites. A statistically significant positive correlation exists between C-isotope and O-isotope values ($r = 0.58$).

The $\delta^{18}O$ isotope composition of the water from which microbialite calcite precipitated was determined using the equations listed below (Epstein *et al.*, 1951; Craig, 1965; Hays & Grossman, 1991; Cerling & Quade, 1993; Kim *et al.*, 2007):

$$1000 \ln\alpha = 16.1\left(10^3\ T^{-1}\right) - 24.6 \qquad (1)$$

$$\alpha = (1000 + \delta_{CaCO_3})/1000 + \delta_{H_2O} \qquad (2)$$

where δ_{CaCO_3} corresponds to the $\delta^{18}O$ of calcite relative to SMOW (Standard Mean Ocean Water) and δ_{H_2O} is the $\delta^{18}O$ of water relative to SMOW:

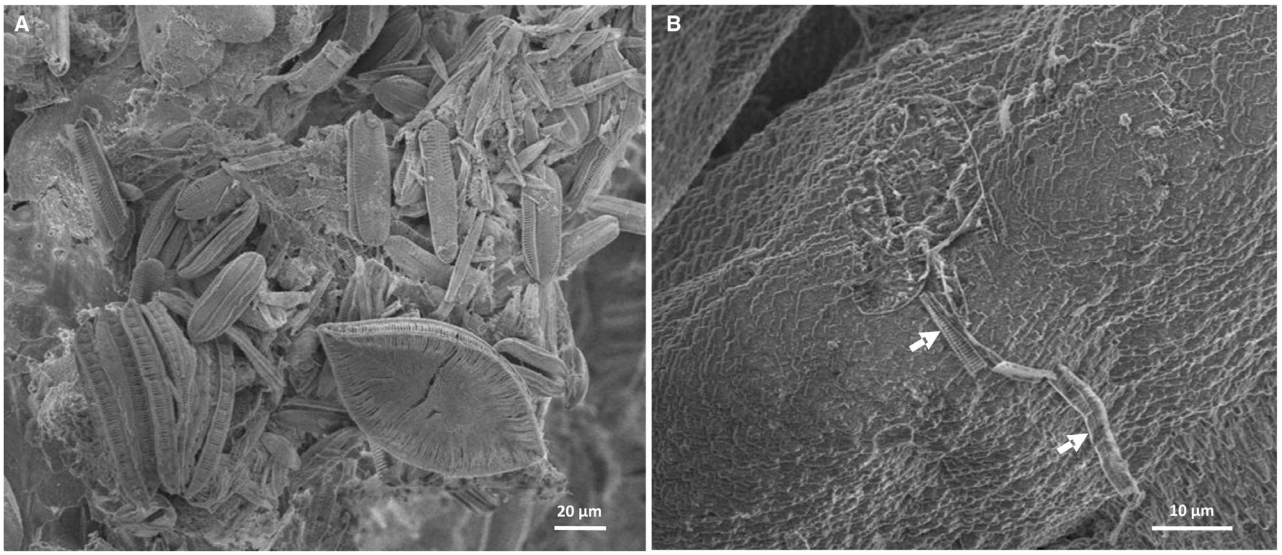

Fig. 5. Scanning electron microscopy (SEM) photomicrographs sample Van-MB-1-1, basal part, Location 1. (A) Mineralized algal mucilage with abundant diatom frustules. (B) Smooth surface of a mat with a diatom frustule (arrows).

$$\delta^{18}O_{calcite}\ (SMOW) = 1.03091 \times \left(\delta^{18}O\ PDB\right) + 30.91 \quad (3)$$

$$\delta^{18}O_{water} = \delta^{18}O_{calcite} - \left(2.78 \times 10^6 / T^2\right) + 2.89 \quad (4)$$

where T is in °K.

The fractionation factor of calcite was used in the above calculations, because the fractionation factors for calcite with different Mg contents are almost identical and aragonite, as a relatively less abundant carbonate mineral in the samples, only shows a small enrichment of 0.6‰ in ^{18}O at 25°C relative to calcite (Tarutani *et al.*, 1969). These calculations used 10°C and 15°C, respectively, representing the upper and lower Lake Van water temperatures for the Spring season, during which the rates of organic carbon flux linked to phytoplankton blooms and the submerged spring activity are at their highest (Reimer *et al.*, 2009; Huguet *et al.*, 2011).

Uranium/thorium ages of microbialites

Measured ^{238}U and ^{232}Th concentrations in studied samples range from *ca* 13 to 21 µg/g and *ca* 150 to 650 ng/g, respectively. Except for four samples, most data are aligned on a horizontal line in a ($^{230}Th/^{232}Th$) versus ($^{238}U/^{232}Th$) plot (i.e. a so-called Rosholt diagram), hence suggesting very recent (< *ca* 0.1 kyr BP) formation (Table S1, Fig. S2). Corresponding ($^{230}Th/^{232}Th$) ratios were significantly higher (*ca* 2.32 ± 0.14; 1 SD; $N = 8$) than secular equilibrium (Table S1), reflecting the addition of excess ^{230}Th from lake water. Therefore, the theoretical end-member used with the isochron method to correct measured U/Th ages for inherited ^{230}Th was extrapolated from the intersection between this regression line and the line for secular equilibrium (Fig. S2; Table S1). The resulting ages of the microbialite chimney at Locations 1 and 2 range from *ca* 0.0 kyr BP to 1.04 kyr BP and *ca* 0.0 kyr BP to 1.00 kyr BP, respectively (Table S1). The ages show no systematic change along the height of the microbialites. Three ages obtained from different parts of a *ca* 50 cm size microbialite sample of chimney 1 in Fig. 3B ranges from *ca* 0.00 kyr BP to 0.64 ± 0.16 kyr.

DISCUSSION

Microbialite formation and evolution

Geological, hydrological and chemical controls. Two competing hypotheses exist for the formation of columnar microbialites (tufa) in alkaline salty lakes, such as Lake Van and Mono Lake in California: (i) they form where Ca-rich groundwater emerges from faults; or (ii) they develop along shorelines where Ca-rich river and groundwater runoff enters the lake (Keevil *et al.*, 2022).

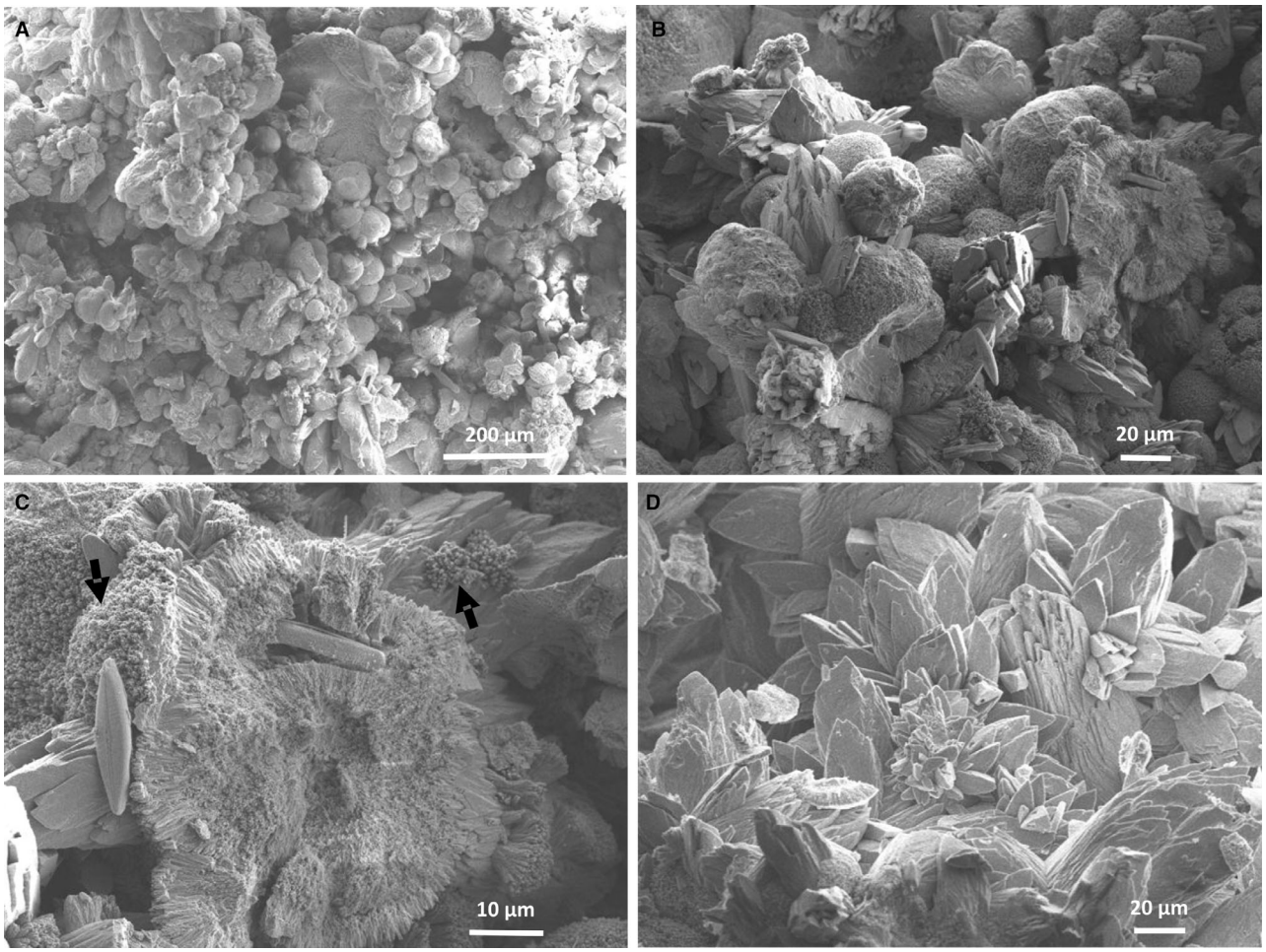

Fig. 6. Scanning electron microscopy (SEM) photomicrographs of microbialite sample Van-MB-2-5, uppermost part, Location 2. (A) Globule aggregates and pore filling, dog-tooth prismatic calcite crystals. (B) Magnified view of the globules with dog-tooth prismatic calcite crystals protruding between the globule aggregates. (C) Concentrically layered internal structure of a globule formed by radial calcite growths. The globule includes pennate diatoms, and its surface is covered by fine cellular growths (<1 µm) (arrows). (D) Close up view of dog-tooth prismatic calcite crystals filling the pore space as cement.

Table 1. Carbonate mineral composition of bulk microbialite samples from Adilcevaz shelf, based on X-ray diffraction (XRD) analysis.

Location/ microbialite sample position	Lab. sample number	Calcite 3.03 Å peak height (cm)	Aragonite 3.39 Å peak height (cm)	Calcite d_{104}-spacing (Å)	Relative calcite percent of total carbonate*
1/Top	Van-MB-1-4	12.8	1.0	3.027	93
2/Upper	Van-MB-2-5	12.2	3.0	3.022	80
2/Middle	Van-MB-2-4	12.4	2.8	3.024	82
2/Lower	Van-MB-2-3	12.4	2.0	3.029	86
2/Above base	Van-MB-2-2	12.7	0.2	3.024	98
2/Basal	Van-MB-2-1	12.5	2.1	3.019	86

*Relative calcite percentage is measured as of the total carbonate percentage, using the peak heights of calcite d_{104} 3.03 Å and to aragonite d_{111} 3.39 Å.

Table 2. Stable isotope analysis of microbialite samples from Adilcevaz shelf.

Location/microbialite sample position	Lab. sample number	$\delta^{18}O_{carb}$ ‰ VPDB	$\delta^{13}C_{carb}$ ‰ VPDB	$\delta^{18}O_{water}$ ‰ VSMOW at 10°C*	$\delta^{18}O_{water}$ ‰ VSMOW at 15°C*
Loc 1/base	Van-MB-1-1	−4.21	3.01	−5.20	−4.01
Loc 1/above base	Van-MB-1-2	−2.90	3.43	−3.85	−2.66
Loc 1/middle	Van-MB-1-3	−3.16	2.96	−4.12	−2.93
Loc 1/uppermost	Van-MB-1-4	−3.61	3.10	−4.58	−3.39
Loc2/base	Van-MB-2-1	−3.96	3.15	−4.95	−3.75
Loc 2/above base	Van-MB-2-2	−5.68	1.91	−6.72	−5.52
Loc 2/lower	Van-MB-2-3	−5.15	2.53	−6.17	−4.98
Loc 2/middle	Van-MB-2-4	−4.94	3.23	−5.95	−4.76
Loc 2/upper	Van-MB-2-5	−5.13	3.36	−6.15	−4.96

*See text for calculation of VSMOW $\delta^{18}O_{water}$ values from $\delta^{18}O_{carb}$ ‰ VPDB.

In Lake Van, our long-term underwater observations and the sub-bottom seismic and multibeam bathymetric data (this study; Cukur *et al.*, 2015; Damcı & Çağatay, 2018) favour the first hypothesis (Fig. 8). The seismic and bathymetric data indicate that the microbialites in the Adilcevaz offshore commonly occur in swarms that are aligned along north-west/south-east and east–west trending normal (extensional) faults, and that their seismically transparent internal parts are due to their porous structure (Fig. 1B and C).

Near the river mouths in the nearshore areas, carbonate precipitation occurs as milky 'whitings' in the surface lake water when Ca-enriched river waters mix with the carbonate-poor, alkaline lake waters (Fig. 8). Mixing between these two different waters results in very high local $CaCO_3$ supersaturation and precipitation. This fine carbonate settles onto the lake floor to form the white laminae of the varved sediments rather than forming tall carbonate chimneys (e.g. Kempe *et al.*, 2002; McCormack *et al.*, 2019). Our dive observations confirm that the microbialite chimneys are formed by focused groundwater flow in central or ancillary channels, with different chimney morphologies (Fig. 2), with focused flow in the central channel forming a columnar morphology (Fig. 2B and C), while flow in ancillary channels forms tree-like, branching morphology (Fig. 2A and D). In contrast, a diffuse groundwater flow through porous sandy sediments mixes with the lake water and forms flat carbonate crust that often acts as a substrate for individual chimneys or chimney swarms (Fig. 2B and E). At such sites, it is most likely that the carbonate encrusted substrate acts as a relatively impervious cap, with focused flow only through some openings that become the site of chimneys and chimney swarms formation.

The rivers draining the area west and north-west of Adilcevaz town, and the submerged springs on the Adilcevaz shelf, are particularly enriched in Ca and bicarbonate ions (Reimer *et al.*, 2009). These ions are sourced mainly from the Miocene Adilcevaz Limestone, which is exposed in outcrops and acts as an important aquifer in the onshore and offshore regions (Figs 1A and 8).

Our stable carbon and oxygen isotope and mineralogical data provide strong supporting evidence for the mixing process between the groundwater and Lake Van surface (epilimnion) waters at the site of microbialites. The ranges of $\delta^{18}O$ values of the waters that precipitated the microbialite carbonates at 10°C and 15°C are −6.72 to −3.85‰ VSMOW and −5.52 to −2.66‰ VSMOW, respectively (Table 2). These values lie between the lake water $\delta^{18}O$ value of −0.1‰ VSMOW, and river and precipitation waters value of −10.8‰ VSMOW (Faber, 1978), strongly supporting the mixing of water masses at the location of studied microbialite chimneys (Fig. 7). Unfortunately, no oxygen isotope data are available for the spring waters emerging on the Adilcevaz shelf. However, the isotope values of the recharging precipitation waters are likely modified by interaction with the Adilcevaz Limestone, having $\delta^{18}O$ values of −5.3‰ to −3.5 VPDB (Çağatay *et al.*, 2014).

The $\delta^{13}C_{DIC}$ composition of Lake Van surface waters has been reported by Kempe *et al.* (1990) and Lemcke (1996), yielding values between 2.7‰ and 5.5‰, respectively. Considering an average calcite–bicarbonate enrichment factor of

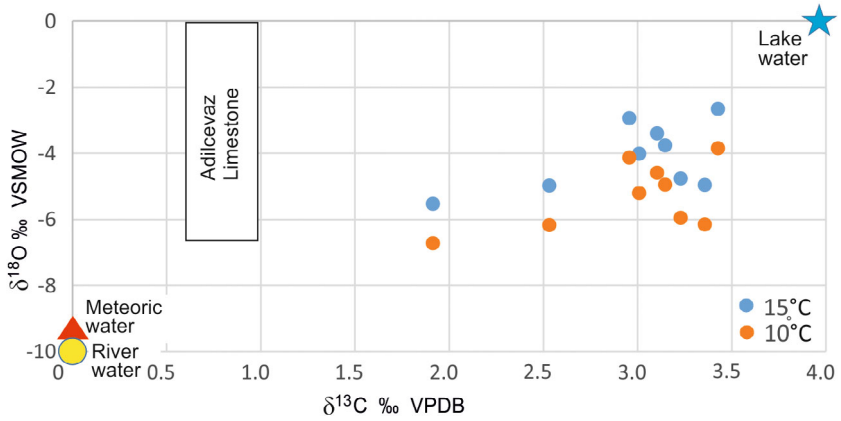

Fig. 7. Plot of calculated carbon and oxygen isotope values for waters from which tufa carbonate was precipitated (this study), compared to those of Lake Van surface water, river water and precipitation water (Faber, 1978), and to those of Adilcevaz Limestone (Çağatay *et al.* (2014). VPDB, Vienna Peedee belemnite; VSMOW, Vienna standard mean ocean water.

1.0‰ over a temperature range of 10 to 40°C (Romanek *et al.*, 1992), the $\delta^{13}C_{carb}$ values (1.91–3.43‰) of Adilcevaz microbialites are compatible with precipitation from surface waters with a $\delta^{13}C_{DIC}$ value of 2.7‰ reported by Lemcke (1996). The higher values reported by Kempe *et al.* (1990) may be due to mixing with deeper water, resulting from weakening of the stratification, and to photosynthetic activity during late summer, at the time of measurement (McCormack *et al.*, 2019).

The predominantly low-Mg calcite mineral composition of the microbialites further suggests that carbonate precipitation took place under low salinity and low Mg/Ca ratio conditions, induced by the sub-lacustrine spring waters, which favoured calcite precipitation over aragonite (Fig. 8) (Mackenzie & Pigott, 1981; Burton & Walter, 1987; De Choudens-Sáanchez & Gonzáalez, 2009; Reimer *et al.*, 2009). This conclusion is supported by the predominance of low-Mg calcite in the dark detrital-rich laminae of Lake Van varved sediments, which is hypothesized to have formed in surface waters under similar temperature and water depth by mixing of Ca-rich (in that case river water) and Ca-poor alkaline lake water during the high spring runoff (McCormack *et al.*, 2019).

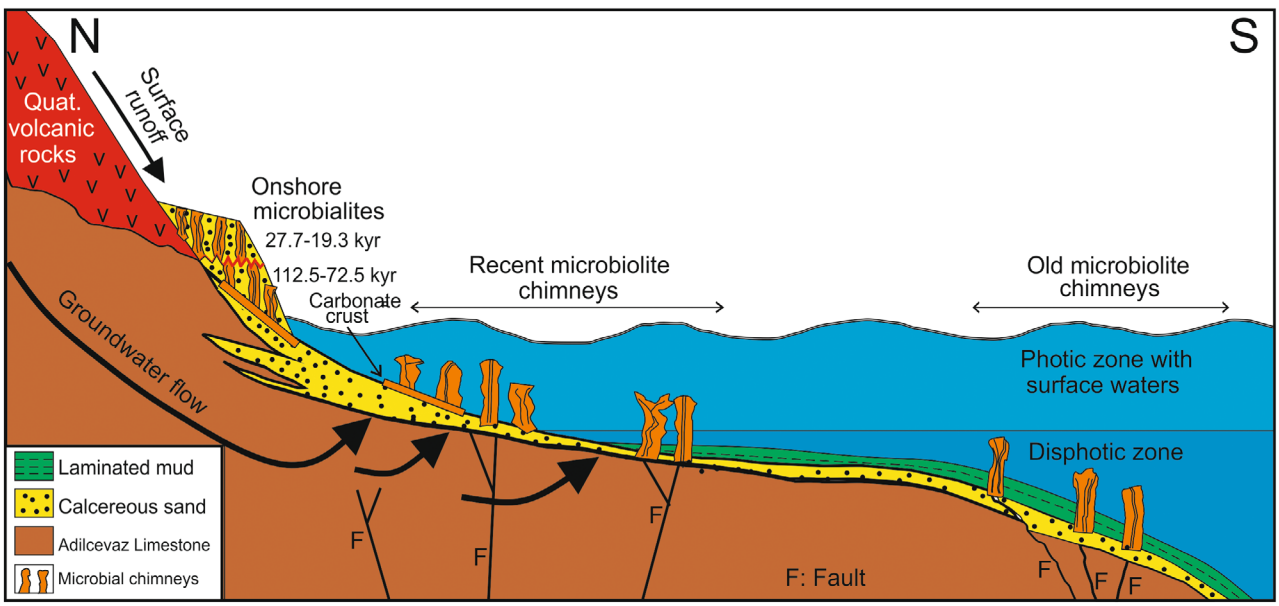

Fig. 8. Schematic cross-section depicting the model of microbialite formation on the northern shelf of Lake Van. Onshore microbialite U/Th age data are from Yeşilova *et al.* (2019).

Age and growth rates of microbialites and links with hydrology and climate. The calculated U/Th ages indicate that the studied microbialites formed very recently, with ages ranging from modern (10 yr) to *ca* 1 kyr BP and six out of 12 ages being modern (Table S1). The U/Th ages do not show any systematic change along the height of the microbialite chimneys and laterally. Three sub-samples derived from sample VAN-MB2-1 yielded ages ranging from modern to 0.64 kyr BP. Such local variability and the evidence for non-systematic changes of U/Th ages along the chimney height both suggest that continuous and active carbonate mineralization occurs along the entire microbialite. Assuming that the sampled 9 m and 15 m high microbialites formed approximately within the last 1 kyr, the authors calculate upward growth rates of 9 to 15 m/kyr. The inferred evidence for fast and active growth of the microbialites is further supported by long-term dive observations that reveal a several centimetres per year growth rate and rapidly engulfed recent artefacts by the carbonate chimneys (Fig. 2F). However, the upward growth rates may be misleading for some microbialites that start to grow laterally or form branches during their development, when the central channel is plugged with inorganic precipitates and organic matter (Fig. 2A and D).

Our fast growth-rate estimates for the submerged Adilcevaz microbialites are roughly comparable with those for tufas exposed in the 24 m thick Adilcevaz onshore sequence (Yeşilova *et al.*, 2019). There, the authors studied two packages of microbialites dated during 112.7 to 72.5 kyr BP and 27.7 to 19.3 kyr BP. The younger package included 14 U/Th dates from nine 0.4 to 1.8 m thick microbialite units, and allowed for growth-rate estimations ranging from 1.2 to 20 m/kyr. However, these estimates are considered to be rather rough, because of the wide error margin of the U/Th ages.

The age span of Lake Van microbialites at water depths of −20 to −25 m offshore Adilcevaz are also comparable with the those from the hypersaline and alkaline Manito Lake in the northern Great Plains of Canada, which formed during 1.3 kyr between about 2.3 kyr BP and 1.0 kyr BP (Last *et al.*, 2010). However, some microbialites elsewhere in the world have formed at even a much faster rate, such as those from Big Soda Lake, Nevada, which grew up to 3 m height in the last 100 yr (Rosen *et al.*, 2004).

In Lake Van and elsewhere in alkaline, salty lakes, the growth rate of microbialites is related to climatically controlled hydrology including lake level variations and/or groundwater discharge rates (e.g. Awramik & Buchheim, 2015; Yeşilova *et al.*, 2019; Ingalls *et al.*, 2022; Keevil *et al.*, 2022). More specifically, the growth rates of microbialites depend on: (i) sustained flow of focused Ca-rich groundwater to the lake; (ii) relatively stable lake water level over the shelf area; and (iii) a balance between growth rate, subsidence rate and lake water level within the photic zone (Fig. 8) (e.g. Awramik & Buchheim, 2015).

Palaeoclimate proxy records of the region such as Lake Van, Lake Zeribar and Dead Sea show that climate was mostly dry during the last 4 kyr, with some lake level oscillations, and relatively drier periods occurred during, 3.5 kyr BP, 2.5 and 0.4 kyr BP (Reimer *et al.*, 2009; Çağatay *et al.*, 2014, and references therein). This is underpinned by the recent palaeoclimatic and archaeological data in the region (Wick *et al.*, 2003; Jacobson *et al.*, 2021; Manning *et al.*, 2023). Moreover, both lake and speleothem studies from Anatolia indicate substantial climate oscillations over the last 2 kyr related to the warm and humid Medieval Climate Anomaly (MCA: *ca* AD 800–1300) and the cold and dry Little Ice Age (LIA: *ca* AD 1500–1750) (Luterbacher *et al.*, 2012; Roberts *et al.*, 2012, and references therein). These climatic changes likely caused water level changes of several metres in Lake Van, as recorded by the submerged palaeo-shorelines of late Holocene age at *ca* 15 m, 25 m and 35 m below the present lake water level offshore Adilcevaz town (Damcı & Çağatay, 2018). Short-term fluctuations in Lake Van level are also indicated by recent data and observations, which show a rise of 4 m between 1963 and 1995 (E.İ.E.İ., 1996, 2008; Meydan *et al.*, 2022) and a drop of *ca* 2 m since 2021.

These recent lake level changes are related to the amount and seasonality of precipitation (Kadıoğlu *et al.*, 1997). Atmospheric precipitation is important for microbialite formation because of its direct controls on groundwater activity, organic activity in the lake's surface waters and the amount of Ca supply to the lake by both surface runoff and groundwater discharge. Hence, the authors consider that the studied 1 kyr old microbialites likely started to evolve mainly during the relatively long warm and humid MCA, when an increase in precipitation promoted high Ca-rich groundwater activity and organic productivity in the photic zone.

Possible lake level drop during the LIA and the more recent 2 m drop have exposed, and even partly eroded, the microbialite chimneys in shallow waters. On the other hand, considering the role for photosynthesis in microbialite formations, rising lake water level would submerge some of the microbialites below the photic zone and stop their development. Hence, microbialites observed in the seismic sections with their tops at water depths greater than −35 m (below photic zone) and those observed on the onshore terraces (Yeşilova *et al.*, 2019) are older, having formed during the earlier transgression periods (Fig. 8).

The role of biological activity and organic matter in driving microbialite growth

This study has examined mainly the internal mineralized part of the submerged microbialites, below the dark living and partly mineralized cyanobacterial crust. Our SEM observations and analyses indicate that the crumbly porous part of microbialites mainly consists of mineralized algal mucilage exhibiting several hundred micron-long tubular organic filaments, together with calcareous globules and elongated prismatic crystals of low-Mg calcite (Figs 3 to 6). The tubular organic filaments are algal material, which are similar to the web-like mineralized organic structures previously observed in microbialites elsewhere in Lake Van (López-García *et al.*, 2005; Kremer *et al.*, 2019) and in Big Soda Lake, Nevada (Rosen *et al.*, 2004) (Fig. 4A to C).

The calcareous globular aggregates are 30 to 40 μm in diameter (Fig. 6A to C) and are replaced by layer by layer calcification of the bacterial organic material (Fig. 6C). They represent benthic coccoid cyanobacteria, as reported earlier in the walls of microbialite axial channels in Lake Van (López-García *et al.*, 2005) and in Silurian black radiolarian cherts as oncoids (e.g. Kremer, 2006) and in Neoarchean (2.8 to 2.5 Ga) stromatolites (Kazmierczak & Altermnn, 2002). The organic matter of algal and extracellular polymeric substances (EPS) of cyanobacterial origin are commonly associated with a dense accumulation of diatom frustules; hence suggesting the important role of both algal and cyanobacterial organic matter in entrapment of skeletal organic matter and inorganic precipitates (Figs 4A, 4C, 5A, 5B and 6C). In experimental studies with alkaline and saline waters, however, similar structures described as fibroradial calcite spherules are formed under a high carbonate mineral saturation state (SI: >2.85) but different alginic acid concentrations (Rogerson *et al.*, 2017; Mercedes-Martín *et al.*, 2021).

The globule surfaces are covered by submicroscopic (<1 μm) rounded and elongated cellular growths of aragonite crystals, rather than the coarser rhombic calcite crystal coatings observed in the experimental studies (Mercedes-Martín *et al.*, 2021). The authors interpret the aragonite crystals as nanoprecipitates or pseudomorphs of 'nanobacteria' associated with coccoid cyanobacteria in Lake Van microbialites (López-García *et al.*, 2005; Benzerara *et al.*, 2006) (Fig. 6C). Such precipitates are also observed in some other modern microbialites, stromatolites and meteorites (Benzerara *et al.*, 2003; Kazmierczak & Kempe, 2003; Rosen *et al.*, 2004; Kremer, 2006; Kremer *et al.*, 2018).

Indeed, DNA analyses of microbialite and lake water extracts in Lake Van have revealed a wide bacterial diversity, especially during spring season due to enhanced inputs of nutrients from regional rivers and spring waters (Huguet *et al.*, 2011). The bacterial assemblages include Proteobacteria, Cyanobacteria, *Cytophaga–Flexibacter–Bacteroides* (CFB) group, Actinobacteria and Firmicutes in microbialites (López-García *et al.*, 2005), and Proteobacteria, Cyanobacteria, Bacteroidota and Firmicutes in water (Ersoy Omeroglu *et al.*, 2021). It is believed that the heterotrophic bacteria promote carbonate precipitation, and thus play a crucial role in the formation of Lake Van microbialites (López-García *et al.*, 2005; Benzerara *et al.*, 2006; Kremer *et al.*, 2019). This assertion is supported by various investigations of modern carbonate sediments and experimental studies, which show that heterotrophic bacteria can mediate $CaCO_3$ precipitation by releasing Ca^{2+} ions from algal and cyanobacterial mucilage and provide a suitable substrate for crystal nucleation (e.g. Knorre & Krumbein, 2000; Paerl & Reid, 2001; Arp *et al.*, 2001; Kawaguchi & Decho, 2002; Lee, 2003; Rodriguez-Navarro *et al.*, 2003; McCutcheon *et al.*, 2016).

Calcite morphogenesis is controlled by carbonate mineral saturation state, Mg/Ca ratio of the parental fluid, and concentration of microbial-derived organic molecules (Rainey & Jones, 2009; Pedley & Rogerson, 2010; Jones & Peng, 2014; Mercedes-Martín *et al.*, 2021, and references therein). Experimental studies simulating alkaline, saline lake settings, such as Lake Van, strongly suggest that the prismatic calcite crystals protruding through the mineralized organic

structures In the Adilcevaz microbialites are inorganic (abiotic) precipitates formed under high saturation index (SI: 2.0–2.6) and low alginic acid concentrations (Fig. 6B and D) (Mercedes-Martín *et al.*, 2021). Both XRD and SEM-EDS analyses indicate that the euhedral calcite is low-Mg calcite, and that the organic framework is replaced mainly by low-Mg calcite and aragonite, with only minor to trace amounts of Mg-silicates (Table 1, Fig. S1).This predominantly carbonate composition of the microbialites is again likely to be due to the carbonate precipitation mainly under the strong influence of the spring waters from the Adilcevaz Limestone aquifer, with high contents of Ca ions as the major cation (Reimer *et al.*, 2009). Additionally, low-Mg calcite precipitation would be locally promoted over high Mg-calcite precipitation by selective chelation/release of Ca ions and exclusion of Mg ions by EPS (Rogerson *et al.*, 2008).

The Adilcevaz shelf microbialites contain only minor to trace amounts of authigenic hydromagnesite, which is in contrast to Mg-rich hyperalkaline lakes such as Lake Alchichica (Mexico), Las Eras (Central Spain) and Lake Salda, southwest Türkiye, where hydromagnesite is a major carbonate phase (Couradeau *et al.*, 2013; Sanz-Montero *et al.*, 2019; Balci *et al.*, 2020). In these Mg-rich lakes, it is proposed on textural evidence that the mineral forms by microbial degradation of EPS under increased pH conditions. A similar mechanism can be envisioned for formation of the minor hydromagnesite in microenvironments of the Adilcevaz microbialites.

In summary, the combination of both textural and structural interpretations discussed above, together with inferences made from dive observations, show that the studied microbialite chimneys formed at locations where focused sublacustrine Ca-rich springs emerge from the lake floor in the photic zone, from the fault zones in the Adilcevaz Limestone aquifer (Fig. 8). The focused outflow induces rapid 'white' carbonate precipitation and high benthic and planktonic algal production and bacterial activity in and around the spring site (Fig. 2D and E). The inorganically precipitated white carbonate around the axial channel is soon covered by cyanobacteria and algal mucilage, especially during the spring season, when freshwater outflow and organic productivity rates are the highest. The growth of the microbialites with a hard and wave resistant structure is facilitated by the entrapment of organic and inorganic materials, and by the microbially mediated mineralization of the cyanobacterial and algal matter (e.g. Arp *et al.*, 2001; Paerl & Reid, 2001; Couradeau *et al.*, 2013; Gerard *et al.*, 2013).

Although some similar microscopic textures, such as the 30 to 40 μm calcareous globules and capsules representative of benthic coccoid cyanobacteria, are present in Lake Van microbialites and Neoarchean stromatolites (2.8 to 2.5 Ga; e.g. Kazmierczak & Altermnn, 2002), the Lake Van microbialites lack the finely laminated structure of the Neoarchean stromatolites, which are believed to have formed under marine conditions rather than in lakes. Therefore, the mechanisms of biocalcification and carbonate precipitation in the widespread and thick Neoarchean stromatolitic carbonates are complicated and debatable issues (Kazmierczak & Altermnn, 2002). However, a role of benthic coccoid cyanobacteria for the biomineralization under alkaline conditions in the stromatolites can be presumed, similar to that observed in the Lake Van microbialites.

The nanobacteria pseudomorphs observed as rounded and elongated aragonite nanocrystals associated with coccoid cyanobacteria in Lake Van microbialites are also observed in meteorites including the Martian ALH84001 meteorite (Benzerara *et al.*, 2003; Kazmierczak & Kempe, 2003). Therefore, alkaline environments and their mixing zones similar to those in Lake Van can be envisioned for the origin of extra-terrestrial life and photosynthetic bacterial activity on Mars (Michalski *et al.*, 2017, and references therein). In particular, Jezero crater has been chosen as a target area for landing and sampling, where an alkaline palaeolake has presumably been in existence (Goudge *et al.*, 2015, 2017; Horgan *et al.*, 2019).

CONCLUDING REMARKS AND PERSPECTIVES

Sub-bottom seismic profiling and dive observations on the northern shelf of Lake Van indicate the presence of up to *ca* 20 m high microbialites aligned along fault and fracture zones, discharging sub-aqueous springs. The microbialites have different morphologies, such as columnar, conical and branching, which form by focused flow of Ca-rich groundwater in central and/or secondary channels. On the contrary diffuse groundwater flow forms flat carbonate crusts on the lake floor.

Below an extensive surficial dark layer of cyanobacteria, the internal carbonate parts of the microbialite chimneys consist predominantly of low-Mg calcite and aragonite, with minor to trace amounts of hydromagnesite. Stable oxygen and carbon isotope measurements indicate that the formation of these microbialites results from the mixing of Ca-rich spring waters emerging from the Adilcevaz Limestone aquifer and Ca-depleted alkaline lake water, fully consistent with dive observations. Microscopic observations reveal that the internal structure of Lake Van microbialites is mediated by bacterially-driven calcification of algal and cyanobacterial mucilage and inorganically precipitated carbonates. According to U/Th analyses, the studied 9 to 15 m high microbialites at 25 m water depth formed during the last millennium, presumably during the warm and humid Medieval Climate Anomaly, when a stable and relatively high lake level existed with a sustained and high groundwater flow rate into the lake. Uranium/Th ages of the subsamples 5 to 6 cm apart, yielding a range of modern to 0.64 kyr ages, as well as the non-systematic changes of ages along the chimney height, suggest continuous and active carbonate mineralization within the entire microbialite. Considering the important role of photosynthesis in their construction, the microbialites observed in the seismic lines at water depth deeper than 35 m likely formed during periods of lake level lower than the present.

Lake Van chimneys represent one of the rare modern analogues of microbial carbonates that existed in early Earth oceans. Hence, the modern Lake Van with its microbialites provides an excellent natural laboratory to elucidate debatable issues related to the physicochemical conditions and biotic and abiotic mineralization processes responsible for the formation of ancient stromatolites and evolution of extra-terrestrial life.

Future field and laboratory investigations will be required to recover deeper microbialites along a north–south depth transect to further explore the age distribution of Lake Van microbiolites and corresponding fluid sources, using for instance strontium (Sr) isotopes, a powerful provenance tracer that can faithfully record the mixing between different fluid sources. Additionally, the distribution of rare earth elements (REE) and other key trace elements in Lake Van microbiolites could be used to investigate not only the composition of ambient source fluids (Webb & Kamber, 2000), but also specific microbial pathways possibly associated with authigenic carbonate precipitation (Bayon *et al.*, 2020). The use of novel environmental proxies will also help with improving our understanding of the biogeochemical processes and microbial mechanisms involved during the precipitation of Lake Van chimneys prior to their application to ancient stromatolitic deposits.

ACKNOWLEDGEMENTS

We acknowledge the funding of the seismic survey by Scientific and Technological Research Council of Türkiye (TÜBİTAK project 108Y279) and the sampling of microbialites by İstanbul Technical University (ITU-BAP Project No. 36595). We thank Dr Ayşegül Feray Meydan and Captain Mete Orhan of Van Yüzüncü Yıl University for their support during the field survey and the sampling campaigns. Emmanuel Ponzevera (IFREMER) is thanked for assistance during MC-ICPMS analyses, and Prof. Gültekin Göller and Engineer Hüseyin Sezer of Metallurgical Engineering Department at ITU for the use of SEM facilities. We acknowledge the constructive criticisms and comments of the two anonymous reviewers and Associate Editor, Mike Rogerson, which considerably improved the paper.

CONFLICT OF INTEREST

The authors declare that they hey have no affiliations with or involvement in any organization or entity with any financial or non-financial (personal) conflicts of interest in the subject matter or materials discussed in this manuscript.

DATA AVAILABILITY STATEMENT

Supplementary data, figures and video of this article can be found at: http://www.emcol.itu.edu.tr/Icerik.aspx?sid=13881.

REFERENCES

Akkuş, M., **Sari, M.**, **Ekmekçi, F.G.** and **Yoğurtçuoğlu, B.** (2021) The discovery of a microbialite-associated freshwater fish in the world's largest saline soda lake, Lake Van (Turkey). *Zoosystem. Evol.*, **97**, 181–189.

Altermann, W. (2004) Precambrian stromatolites: problems in definition, classification, morphology and stratigraphy. In: *The Precambrian Earth: Tempos and Events* (Eds Eriksson, P.G., Altermann, W., Nelson, D.R., Mueller, W.U. and Catuneanu, O.), pp. 564–574. Elsevier, Amsterdam.

Arp, G., **Reimer, A.** and **Reitner, J.** (2001) Photosynthesis-induced biofilm calcification and calcium concentrations in Phanerozoic oceans. *Science*, **292**, 1701–1704.

Awramik, S. and **Buchheim, P.** (2015) Giant stromatolites of the Eocene Green River Formation (Colorado, USA). *Geology*, **43**, 691–694.

Balci, N., **Gunes, Y.**, **Kaiser, J.**, **Akcer On, S.**, **Eris, E.**, **Garczynski, B.** and **Horgan, B.H.N.** (2020) Biotic and abiotic imprints on Mg-Rich stromatolites: lessons from Lake Salda, SW, Turkey. *Geomicrobiol. J.*, **37**, 401–425.

Bayon, G., **Henderson, G.M.** and **Bohn, M.** (2009) U-Th stratigraphy of a cold seep carbonate crust. *Chem. Geol.*, **260**, 47–56.

Bayon, G., **Dupré, S.**, **Ponzevera, E.**, **Etoubleau, J.**, **Chéron, S.**, **Pierre, C.**, **Mascle, J.**, **Boetius, A.** and **de Lange, G.** (2013) Formation of carbonate chimneys in the Mediterranean Sea linked to deep-water oxygen depletion. *Nat. Geosci.*, **6**, 755–760.

Bayon, G., **Henderson, G.M.**, **Etoubleau, J.**, **Caprais, J.-C.**, **Ruffine, L.**, **Marsset, T.**, **Dennielou, B.**, **Cauquil, E.**, **Voisset, M.** and **Sultan, N.** (2015) U-Th isotope constraints on gas hydrate and pockmark dynamics at The Niger Delta margin. *Mar. Geol.*, **370**, 87–98.

Bayon, G., **Lemaitre, N.**, **Barrat, J.A.**, **Wang, X.**, **Feng, D.** and **Duperron, S.** (2020) Microbial utilization of rare earth elements at cold seeps related to aerobic methane oxidation. *Chem. Geol.*, **555**, 119832.

Benzerara, K., **Menguy, N.**, **Guyot, F.**, **Dominici, C.** and **Gillet, P.** (2003) Nanobacteria-like calcite single crystals at the surface of the Tataouine meteorite. *Proc. Natl. Acad. Sci. U. S. A.*, **100**, 7438–7442.

Benzerara, K., **Menguy, N.**, **Lopez-Garcia, P.**, **Yoon, T.-H.**, **Kazmierczak, J.**, **Tyliszczak, T.**, **Guyot, F.** and **Brown, E.J., Jr.** (2006) Nanoscale detection of organic signatures in carbonate microbialites. *Proc. Natl. Acad. Sci. USA*, **103**, 9440–9445.

Bischoff, J.L., **Stine, S.**, **Rosenbauer, R.J.**, **Fitzpatrick, J.A.** and **Stafford, T.W., Jr.** (1993) Ikaite precipitation by mixing of shoreline springs and lake water, Mono Lake, California, USA. *Geochim. Cosmochim. Acta*, **57**, 3855–3865.

Brasier, A., **Wacey, D.**, **Rogerson, M.**, **Guagliardo, P.**, **Saunders, M.**, **Kellner, S.** and **Reijmer, J.** (2018) A microbial role in the construction of Mono Lake carbonate chimneys? *Geobiology*, **16**, 540–555.

Burton, E.A. and **Walter, L.M.** (1987) Relative precipitation rates of aragonite and Mg calcite from seawater: temperature or carbonate ion control? *Geology*, **15**, 111–114.

Çağatay, M.N., **Öğretmen, N.**, **Damcı, E.**, **Stockhecke, M.**, **Sancar, Ü.**, **Eris, K.K.** and **Özeren, S.** (2014) Lake level and climate records of the last 90 ka from the Northern Basin of Lake Van, eastern Turkey. *Quat. Sci. Rev.*, **104**, 97–116.

Cerling, T.E. and **Quade, J.** (1993) Stable carbon and oxygen isotopes in soil carbonates. In: *Climate Change in Continental Isotopic Records* (Eds Swart, P.K., Lohmann, K.C., Mckenzie, J. and Savin, S.), *Geophysical Monograph Series*, **78**, 217–231.

Chafetz, H.S. and **Buczynski, C.** (1992) Bacterially induced lithification of microbial mats. *Palaios*, **7**, 277–293.

Cheng, H., **Adkins, J.**, **Edwards, R.L.** and **Boyle, E.A.** (2000) U-Th dating of deep-sea corals. *Geochim. Cosmochim. Acta*, **64**, 2401–2416.

Council, T.C. and **Bennett, P.C.** (1993) Geochemistry of ikaite formation at Mono Lake, California: Implications for the origin of tufa mounds. *Geology*, **21**, 971–974.

Couradeau, E., **Benzerara, K.**, **Gérard, E.**, **Estéve, I.**, **Moreira, D.**, **Tavera, R.** and **López-García, P.** (2013) Cyanobacterial calcification in modern microbialites at the submicrometer scale. *Biogeosciences*, **10**, 5255–5266.

Craig, H. (1965) The measurement of oxygen palaeoteomperatures. In: *Stable Isotopes in Oceanographic Studies and Palaeotemperatures*. (Ed. Tongiorgi, E.), *C.N.R. Lab. Geol. Nucleare, Pisa*, **80**, 161–182.

Cukur, D., **Krastel, S.**, **Çağatay, M.N.**, **Damcı, E.**, **Meydan, A.F.** and **Kim, S.** (2015) Evidence of extensive carbonate mounds and sublacustrine channels in shallow waters of Lake Van, eastern Turkey, based on high-resolution chirp subbottom profiler and multibeam echosounder data. *Geo-Mar. Lett.*, **35**, 329–340.

Damcı, E. and **Çağatay, M.N.** (2018) Evolution of some morphological, tectonic and volcanic features in Lake Van, based on correlation of seismic and core data. *Quat. Int.*, **486**, 29–43.

De Choudens-Sáanchez, V. and **Gonzáalez, L.A.** (2009) Calcite and aragonite precipitation under controlled instantaneous supersaturation: elucidating the role of $CaCO_3$ saturation state and Mg/Ca ratio on calcium carbonate polymorphism. *J. Sediment. Res.*, **79**, 363–376.

Dekov, V.M., **Egueha, N.M.**, **Kamenov, G.D.**, **Bayon, G.**, **Lalonde, S.V.**, **Schmidt, M.** and **Liebetrau, V.** (2014) Hydrothermal carbonate chimneys from a continental rift (Afar Rift): Mineralogy, geochemistry, and mode of formation. *Chem. Geol.*, **387**, 87–100.

E.İ.E.İ (1996) *Lake Levels*. Elektrik İdaresi Etüt İşleri Genel Müdürlüğü Yayını, Ankara (in Turkish).

E.İ.E.İ (2008) *Lake Levels*. Elektrik İdaresi Etüt İşleri Genel Müdürlüğü Yayını, Ankara (in Turkish).

Epstein, S., **Buchsbaum, R.**, **Lowenstam, H.A.** and **Urey, H.C.** (1951) Carbonate-water isotopic temperature scale. *Bull. Geol. Soc. Am.*, **62**, 417–426.

Ersoy Omeroglu, E., **Sudagidan, M.**, **Zafer-Yurt, M.N.**, **Tasbasi, B.B.**, **Acar, E.E.** and **Ozalp, V.C.** (2021) Microbial community of soda Lake Van as obtained from direct and enriched water, sediment and fish samples. *Nat. Sci. Rep.*, **11**, 18364.

Faber, E. (1978) Oxygen isotope study of Lake Van sediments and waters. In: *Geology of Lake Van* (Eds Degens, E.T. and Kurtman, F.). M.T.A. Press, Ankara.

Folk, R.L. (1993) SEM imaging of bacteria and nannobacteria in carbonate sediments and rocks. *J. Sed. Petrol.*, **63**, 990–999.

Gerard, E., **Menez, B.**, **Couradeau, E.**, **Moreira, D.**, **Benzerara, K.** and **López-García, P.** (2013) Combined three-dimensional Raman and molecular fluorescence imaging reveal specific carbonatemicrobe interactions in modern microbialites. *ISME J.*, **7**, 1997–2009.

Goldsmith, J.R., **Graf, D.L.** and **Heard, H.C.** (1961) Lattice constants of the calcium-magnesium carbonates. *Am. Mineral.*, **46**, 453–457.

Goudge, T.A., **Aureli, K.L.**, **Head, J.W.**, **Fassett, C.I.** and **Mustard, J.F.** (2015) Classification and analysis of

candidate impact crater-hosted closed basin lakes on Mars. *Icarus*, **260**, 336–346.

Goudge, T.A., **Milliken, R.E.**, **Head, J.W.**, **Mustard, J.F.** and **Fassett, C.** (2017) Sedimentological evidence for a deltaic origin of the western fan deposit in Jezero crater, Mars and implications for future exploration. *Earth Planet. Sci. Lett.*, **458**, 357–365.

Grotzinger, J.P. and **Knoll, A.H.** (1999) Stromatolites in Precambrian carbonates: evolutionary mileposts or environmental dipsticks? *Annu. Rev. Earth Planet. Sci.*, **27**, 313–358.

Hays, P.D. and **Grossman, E.L.** (1991) Oxygen isotopes in meteoric calcite cements as indicators of continental paleoclimate. *Geology*, **19**, 441–444.

Horgan, B., **Anderson, R.**, **Dromart, G.**, **Amador, E.** and **Rice, M.** (2019) The mineral diversity of Jezero crater: evidence for possible lacustrine carbonates. *Icarus*, **339**, 113526.

Huguet, C., **Fietz, S.**, **Stockhecke, M.**, **Sturm, M.**, **Anselmetti, F.S.** and **Rosell-Melé, A.** (2011) Biomarker seasonality study in Lake Van, Turkey. *Org. Geochem.*, **42**, 1289–1298.

Ingalls, M., **Fetrow, A.C.**, **Snell, K.E.**, **Frantz, C.M.** and **Trower, E.J.** (2022) Lake level controls the recurrence of giant stromatolite facies. *Sedimentology*, **69**, 1649–1674.

Jacobson, M.J., **Flohr, P.**, **Gascoigne, A.**, **Leng, M.J.**, **Sadekov, A.**, **Cheng, H.**, **Tüysüz, O.** and **Fleitmann, D.** (2021) Heterogenous Late Holocene Climate in the Eastern Mediterranean—The Kocain Cave Record From SW Turkey. *Geophys. Res. Lett.*, **48**, e2021GL094733.

Jones, B. and **Peng, X.** (2014) Signatures of biologically influenced $CaCO_3$ and Mg–Fe silicate precipitation in hot springs: case study from the Ruidian geothermal area, western Yunnan Province, China. *Sedimentology*, **61**, 56–89.

Kadıoğlu, M., **Sen, Z.** and **Batur, E.** (1997) The greatest soda-water lake in the world and how it is influenced by climatic change. *Ann. Geophys.*, **15**, 1489–1497.

Kavak, M.T. and **Karadogan, S.** (2012) Investigation of surface water temperature variation of Lake Van using satellite data. IV. Uzaktan Algılama ve Cografi Bilgi Sistemleri Sempozyumu (UZAL-CBS 2012), 16–19 November 2012, Zonguldak, Turkey (in Turkish).

Kawaguchi, T. and **Decho, A.W.** (2002) A laboratory investigation of cyanobacterial extracellular polymeric secretions (EPS) in influencing $CaCO_3$ polymorphism. *J. Cryst. Growth*, **240**, 230–235.

Kazmierczak, J. and **Altermnn, W.** (2002) Neoarchean biomineralization by benthic cynaobacteria. *Science*, **298**, 2351.

Kazmierczak, J. and **Kempe, S.** (2003) Modern terrestrial analogues for the carbonate globules in Martian meteorite ALH84001. *Naturwissenschaften*, **90**, 167–172.

Kazmierczak, J., **Kempe, S.** and **Altermann, W.** (2004) Microbial origin of Precambrian carbonates: lessons from modern analogues. In: *The Precambrian Earth: Tempos and Events* (Eds Eriksson, P.G., Altermann, W., Nelson, D.R., Mueller, W.U. and Catuneanu, O.), pp. 545–556. Elsevier, Amsterdam.

Keevil, C.E., **Rogerson, M.**, **Parsons, D.**, **Mercedes-Martin, R.**, **Brasier, A.T.**, **Reijmer, J.J.G.** and **Matthews, A.** (2022) The geomorphological distribution of subaqueous tufa columns within a hypersaline lake: Mono Lake, USA. *J. Sediment. Res.*, **92**, 530–545.

Kempe, S., **Landmann, G.**, **Konuk, T.** and **Düzbastılar, M.** (1990) Berichte zur 3. Internationalen Van See Expedition 7. Juni bis 6. Juli 1990. https://doi.org/10.13140/RG.2.2.12966.93767.

Kempe, S., **Kazmierczak, J.**, **Landmann, G.**, **Konuk, T.**, **Reimer, A.** and **Lipp, A.** (1991) Largest known mikrobialites discovered in Lake Van, Turkey. *Nature*, **349**, 605–608.

Kempe, S., **Landmann, G.** and **Müller, G.** (2002) A floating varve chronology from the last glacial maximum terrace of Lake Van/Turkey. *Res. Deserts Mt. Afr. Cent. Asia*, **126**, 97–114.

Kim, S.T., **Mucci, A.** and **Taylor, B.** (2007) Phosphoric acid fractionation factors for calcite and aragonite between 25 and 75°C: revisited. *Chem. Geol.*, **246**, 135–146.

Kipfer, R., **Baur, A.-H.W.**, **Hofer, H.**, **Imboden, D.M.** and **Signer, P.** (1994) Injection of mantle type helium into Lake Van (Turkey): the clue for quantifying deep water renewal. *Earth Planet. Sci. Lett.*, **125**, 357–370.

Knorre, H. and **Krumbein, W.E.** (2000) Bacterial calcification. In: *Microbial Sediments* (Eds Riding, R.E. and Awramik, S.M.), pp. 25–31. Springer, Berlin.

Kremer, B. (2006) Mat−forming coccoid cyanobacteria from early Silurian marine deposits of Sudetes, Poland. *Acta Palaeontologica Polonica*, **51**, 143–154.

Kremer, B., **Kaźmierczak, J.** and **Srodoń, J.** (2018) Cyanobacterial-algal crusts from Late Ediacaran paleosols of the East European Craton. *Precambrian Res.*, **305**, 236–246.

Kremer, B., **Kazmierczak, J.** and **Kempe, S.** (2019) Authigenic replacement of cyanobacterially precipitated calcium carbonate by aluminium silcates in giant microbialites of Lake Van (Turkey). *Sedimentology*, **66**, 285–304.

Last, F.M., **Last, W.M.** and **Halden, N.M.** (2010) Carbonate microbialites and hardgrounds from Manito Lake, an alkaline, hypersaline lake in the northern Great Plains of Canada. *Sediment. Geol.*, **225**, 34–49.

Lee, Y.N. (2003) Calcite production by Bacillus amyloquefaciens CMB01. *J Microbiol.*, **41**, 345–348.

Lemcke, G. (1996) *Paläoklimarekonstruktion am Van See (Ostanatolien, Türkei)*. Doctoral dissertation. ETH, Zürich. 182 pp., unpublished.

López-García, P., **Kaźmierczak, J.**, **Benzerara, K.**, **Kempe, S.**, **Guyot, F.** and **Moreira, D.** (2005) Bacterial diversity and carbonate precipitation in the giant microbialites from the highly alkaline Lake Van, Turkey. *Extremophiles*, **9**, 263–274.

Ludwig, K.R. (2008) Using Isoplot/Ex, version 3.70. A geochronological toolkit for microsoft excel. *Berkeley Geochronol. Ctr. Spec. Pub.*, **20**, 4.

Luterbacher, J., **García-Herrera, R.**, **Akcer-On, S.**, **Allan, R.**, **Alvarez-Castro, M.C.**, **Benito, G.**, **Booth, J.**, **Büntgen, U.**, **Cagatay, N.**, **Colombaroli, D.**, **Davis, B.**, **Esper, J.**, **Felis, T.**, **Fleitmann, D.**, **Frank, D.**, **Gallego, D.**, **Garcia-Bustamante, E.**, **Glaser, R.**, **Gonzalez-Rouco, F.J.**, **Goosse, H.**, **Kiefer, T.**, **Macklin, M.G.**, **Manning, S.W.**, **Montagna, P.**, **Newman, L.**, **Power, M.J.**, **Rath, V.**, **Ribera, P.**, **Riemann, D.**, **Roberts, N.**, **Sicre, M.A.**, **Silenzi, S.**, **Tinner, W.**, **Tzedakis, P.C.**, **Valero-Garcés, B.**, **van der Schrier, G.**, **Vannière, B.**, **Vogt, S.**, **Wanner, H.**, **Werner, J.P.**, **Willett, G.**, **Williams, M.H.**, **Xoplaki, E.**, **Zerefos, C.S.** and **Zorita, E.** (2012) A review of 2000 years of paleoclimatic evidence in the Mediterranean. In: *The Climate of the Mediterranean Region: From the Past to the Future* (Ed Lionello, P.), pp. 87–185. Elsevier, Amsterdam.

Mackenzie, F.T. and **Pigott, J.D.** (1981) Tectonic controls of Phanerozoic sedimentary rock cycling. *J. Geol. Soc. London*, **138**, 183–196.

Manning, S.W., **Kocik, C.**, **Lorentzen, B.** and **Sparks, J.P.** (2023) Severe multi-year drought coincident with Hittite collapse around 1198–1196 BC. *Nature*, **1-6**, 719–724.

McCormack, J., **Nehrke, G.**, **Jöns, N.**, **Immenhauser, A.** and **Kwiecien, O.** (2019) Refining the interpretation of lacustrine carbonate isotope records: Implications of a mineralogy-specific Lake Van case study. *Chem. Geol.*, **513**, 167–183.

McCutcheon, J., **Nothdurft, L.D.**, **Webb, G.E.**, **Paterson, D.** and **Southam, G.** (2016) Beachrock formation via microbial dissolution and re-precipitation of carbonate minerals. *Mar. Geol.*, **382**, 122–135.

Mercedes-Martín, R., **Rogerson, M.**, **Prior, T.**, **Brasier, A.T.**, **Reijmer, J.J.G.**, **Billing, I.**, **Matthews, A.**, **Love, T.**, **Lepley, S.** and **Pedley, M.** (2021) Towards a morphology diagram for terrestrial carbonates: evaluating the impact of carbonate supersaturation and alginic acid in calcite precipitate morphology. *Geochim. Cosmochim. Acta*, **306**, 340–361.

Merz, M. (1992) The biology of carbonate precipitation by cyanobacteria. *Facies*, **26**, 81–102.

Meydan, A.F., **Akkol, S.** and **Doğan, O.N.** (2022) Implications from the meteorological data effects. *Bulletin*, **11**, 299–308.

Michalski, J.R., **Onstott, T.C.**, **Mojzsis, S.J.**, **Mustard, J.**, **Chan, Q.**, **Niles, P.B.** and **Stewart Johnson, S.** (2017) The Martian subsurface as a potential window into the origin of life. *Nat. Geosci.*, **11**, 21–26. https://www.researchgate.net/publication/343219935.

Paerl, H.W., **Steppe, T.F.** and **Reid, R.P.** (2001) Bacterially mediated precipitation in marine stromatolites. *Environ. Microbiol.*, **3**, 123–130.

Pedley, H.M. and **Rogerson, M.** (2010) In vitro investigations of the impact of different temperature and flow velocity conditions on tufa microfabric. *Geol. Soc. Lond. Spec. Publ.*, **336**, 193–210.

Pedone, V.A. and **Folk, R.L.** (1996) Formation of aragonite cement by nannobacteria in the Great Salt Lake, Utah. *Geology*, **24**, 763–765.

Pentecost, A. and **Bauld, J.** (1988) Nucleation of calcite on the sheaths of cyanobacteria using a simple diffusion cell. *Geomicrobiol J.*, **6**, 129–135.

Reimer, A., **Landmann, G.** and **Kempe, S.** (2009) Lake Van, eastern Anatolia, hydrochemistry and history. *Aquat Geochem.*, **15**, 195–222.

Rainey, D.K. and **Jones, B.** (2009) Abiotic versus biotic controls on the development of the Fairmont Hot Springs carbonate deposit, British Columbia, Canada. *Sedimentology*, **56**, 1832–1857.

Reitner, J., Quéric, N.V. and **Arp, G.** (Eds) (2011) *Advances in Stromatolite Geobiology*, p. 560. Springer, Berlin & Heidelberg.

Riding, R. (1982) Cyanophyte calcification and changes in ocean chemistry. *Nature*, **299**, 814–815.

Roberts, N., **Moreno, A.**, **Valero-Garcés, B.L.**, **Corella, J.P.**, **Jones, M.**, **Allcock, S.**, **Woodbridge, J.**, **Morellón, M.**, **Luterbacher, J.**, **Xoplaki, E.** and **Türkeş, M.** (2012) Palaeolimnological evidence for an east-west climate see-saw in the Mediterranean since AD 900. *Global Planet. Change*, **84–85**, 23–34.

Rodriguez-Navarro, C., **Rodriguez-Gallego, M.**, **Ben Chekroun, K.** and **Gonzalez-Munoz, M.T.** (2003) Conservation of ornamental stone by Myxococcus xanthus-induced carbonate biomineralization. *Appl. Environ. Microbiol.*, **69**, 2182–2193.

Rogerson, M., **Pedley, H.M.**, **Wadhawan, J.D.** and **Middleton, R.** (2008) New insights into biological influence on the geochemistry of freshwater carbonate deposits. *Geochim. Cosmochim. Acta*, **72**, 4976–4987.

Rogerson, M., **Mercedes-Martín, R.**, **Brasier, A.T.**, **McGill, R.A.**, **Prior, T.J.**, **Vonhof, H.**, **Fellows, S.M.**, **Reijmer, J.J.G.**, **McClymont, E.**, **Billing, I.**, **Matthews, A.** and **Pedley, M.** (2017) Are spherulitic lacustrine carbonates an expression of large-scale mineral carbonation? A case study from the East Kirkton Limestone, Scotland. *Gondw. Res.*, **48**, 101–109.

Romanek, C.S., **Grossman, E.L.** and **Morse, J.W.** (1992) Carbon isotopic fractionation in synthetic aragonite and calcite: effects of temperature and precipitation rate. *Geochim. Cosmochim. Acta*, **56**, 419–430.

Rosen, M.R., **Arehart, G.B.** and **Lico, M.S.** (2004) Exceptionally fast growth rate of <100-yr-old tufa, Big Soda Lake,Nevada: implications for using tufa as a paleoclimate proxy. *Geology*, **32**, 409–412.

Salvatore, M.R., **Goudge, T.A.**, **Bramble, M.S.**, **Edwards, C.S.**, **Bandfield, J.L.**, **Amador, E.S.**, **Mustard, J.F.** and **Christensen, P.R.** (2018) Bulk mineralogy of the NE Syrtis and Jezero crater regions of Mars derived through thermal infrared spectral analyses. *Icarus*, **301**, 76–96.

Sanz-Montero, M.E., **Cabestrero, O.** and **Mónica, S.-R.M.** (2019) Microbial Mg-rich Carbonates in an Extreme Alkaline Lake (Las Eras, Central Spain). *Front. Microbiol.*, **10**, 148.

Sarı, M. (2008) Threatened fishes of the world: *Chalcalburnus tarichi* (Pallas 1811) (Cyprinidae) living in the highly alkaline Lake Van, Turkey. *Environ. Biol. Fishes*, **81**, 21–23.

Stockhecke, M., **Anselmetti, F.S.**, **Meydan, A.F.**, **Odermatt, D.** and **Sturm, M.** (2012) The annual particle cycle in Lake Van (Turkey). *Palaeogeogr. Palaeoclimatol. Palaeoecol.*, **333-334**, 148–159.

Tarutani, T., **Clayton, R.N.** and **Mayeda, T.K.** (1969) The effect of polymorphism and magnesium substitution on oxygen isotope fractionation between calcium carbonate and water. *Geochim. Cosmochim. Acta*, **33**, 987–996.

Webb, G.E. and **Kamber, B.S.** (2000) Rare earth elements in Holocene reefal microbialites: a new shallow seawater proxy. *Geochim. Cosmochim. Acta*, **64**, 1557–1565.

Wick, L., **Lemcke, G.** and **Sturm, M.** (2003) Evidence of Lateglacial and Holocene climatic change and human impact in eastern Anatolia: high-resolution pollen, charcoal, isotopic and geochemical records from the laminated sediments of Lake Van, Turkey. *Holocene*, **3**, 665–675.

Wong, H.K. and **Finckh, P.** (1978) Shallow structures in Lake Van. In: *Geology of Lake Van* (Eds Degens, E.T. and Kurtman, F.), pp. 20–27. M.T.A. Press, Ankara.

Wright, V.P. and **Barnett, A.J.** (2015) An abiotic model for the development of textures in some South Atlantic early Cretaceous lacustrine carbonates. In: *Microbial Carbonates in Space and Time: Implications for Global Exploration and Production, vol. 418* (Ed Bosence, D.W.J.). Geological Society of London Special Publication, London.

Wunderlich, J. and **Müller, S.** (2003) High-resolution sub-bottom profiling using parametric acoustics. *Int. Ocean Syst.*, **7**, 6–11.

Yeşilova, Ç., **Gülyüz, E.**, **Huang, C.-R.** and **Shen, C.-C.** (2019) Giant tufas of Lake Van record lake-level fluctuations and climatic changes in eastern Anatolia, Turkey. *Palaeogeogr., Palaeoclimatol., Palaeoecol.*, **533**, 109226.

Manuscript received 20 February 2023; revision accepted 25 October 2023

Supporting Information

Additional information may be found in the online version of this article:

Figure S1. X-ray diffractograms of two representative microbialite samples. Cu K_α radiation.

Figure S2. Rosholt diagram for Lake Van microbialites. The green dotted line represents the equiline (secular equilibrium).

Table S1. Measured U/Th data (+2 s) for Lake Van microbialite carbonate samples and activity ratios used for isochron age calculation.

Video S1. An underwater video from Adilcevaz shelf showing an active chimney at *ca* 5 m water depth, discharging freshwater and precipitating white soft carbonates.